Discrete fracture-matrix model of poroelasticity

Jan Březina and Jan Stebel

Institute of New Technologies and Applied Informatics
Faculty of Mechatronics, Informatics and Interdisciplinary Studies
Technical University of Liberec
Studentská 1402/2, 461 17 Liberec, Czech Republic
{jan.brezina,jan.stebel}@tul.cz

November 24, 2023

Abstract

The paper presents the derivation and analysis of a poroelasticity model in a domain with fracture represented by a codimension-one manifold. The system of saturated flow and linear elasticity both in the rock matrix and in the fracture coupled through appropriate interface condition is obtained from a continuum description by integration and semi-discretization in the normal direction of the fracture. The existence and uniqueness of a weak solution are proved with the help of an iterative splitting, whose convergence rate is analyzed. The analysis is complemented by a numerical example.

Keywords: Biot's poroelasticity, discrete fracture-matrix model, fixed-stress splitting.

2010 Mathematics Subject Classification: 35M33, 35Q86, 74S05, 74F10.

1 Introduction

The hydromechanical (HM) interaction of fluid flow and rock mechanics plays a significant role in many important applications such as geothermal power utilization, nuclear waste deposition, or CO_2 storage [35]. Rocks, in which these facilities are located, are characterized by the presence of fracture networks. The size of individual fractures varies from a sub-milimeter scale (grain size cracks) to a kilometer-scale (fault zones) [8]. Mathematical modelling of such systems is a challenging task involving coupled physical processes at different geometrical scales. As the fracture apertures are still far from the scale of individual molecules, the continuum models of the HM processes derived from fundamental conservation laws are physically reasonable. Currently, there exist three types of approaches to treating fractures in continuum-based models [4]: equivalent continuum, discrete fracture networks (DFN) and discrete fracture-matrix (DFM) models.

In equivalent continuum models, the influence of small-scale fractures is incorporated into the macroscopic properties of the rock, such as the permeability [33, 36]. However, the very high aspect ratio (size over aperture) of the fractures leads to large gradients of the principal unknowns, typically flow velocity and displacement, that cannot be resolved by classical discretization methods (FVM, FEM).

On the other hand, the *discrete fracture network* (DFN) approach [17, 26] that describes individual fractures as codimension-one manifolds is unable to treat a vast number of small-scale fractures. Various hybrid approaches are used to combine continuum and discrete fractures; we refer to [27] for an overview and to [45] for a numerical comparison of selected approaches.

The *discrete fracture-matrix* (DFM) models, also called *mixed-dimensional*, are derived from the continuum model by a *semi-discretization* of the governing equations on the fracture domain in the normal direction. The fracture domain of the resulting equations is reduced to a codimension-one manifold, similarly to the DFN approach. The reduction of the fracture domain's dimension leads some authors to name the process *dimension reduction*. However, that term has a quite different meaning in the data processing. In order to avoid confusion, we rather use the term semi-discretization further on. This technique was used by Martin et al. [29] for Darcy flow equations in domains with a single fracture. Later, the model was extended by [1] for immersed, polygonal fracture with variable aperture. The models with intersections and junctions and extension to the transport problems were analyzed in [30, 34, 18, 37, 25].

A classical approach for the HM coupling is based on the linear poroelastic model introduced by Biot [5] or some of its more recent non-linear extensions [35, 28]. Poroelasticity models coupled to discrete fracture flow, neglecting the mechanical response of the fractures, were studied e.g., in [20, 22, 23, 14, 24]. Fracture mechanics, however, plays an important role in the applications. Natural fractures are never smooth, and can be filled by solid material e.g. due to healing [40]. Hence fracture stiffness, non-penetration and friction conditions have to be taken into account. Fracture stiffness can be estimated using rock joint models [2], see also [35]. There has been an ongoing research on the numerical analysis and simulation of models involving fracture contact mechanics, see e.g. [21, 19, 3, 6, 7]. In these works, the fracture stiffness is not considered. Recently, a general framework for nonlinear poromechanics in the mixed-dimensional setting was presented and rigorously analyzed in [9]. The authors showed that their DFM model includes as special cases several models obtained by semi-discretization. In the case of poroelasticity with non-void fractures it is however not clear, whether both approaches are equivalent. We also mention the work [31], where a shell model is derived for a poroelastic membrane.

The purpose of the present paper is threefold:

1. We derive the DFM model of poroelasticity using the semi-discretization process for the Biot system. In order to keep the subsequent analysis reasonably demanding, we do not consider the nonlinear effects on fracture-matrix interface (such as contact, friction, and displacement-dependent conductivity). This makes the resulting model valid only in the case of small variations of fracture aperture. We also restrict ourselves to the case of a single fracture. We refer to [39] where we present a more complex

numerical model with fracture network and nonlinear fracture poromechanics. To cope with the fact that the mechanical part (2.1a) of the problem is a vector-valued problem, we develop a particular calculus for tangential and normal parts of functions and operators. In contrast to other works, we consider general conductivity and elasticity tensors not necessarily aligned with the fracture orientation. The obtained equations are expressed in terms of mean pressure and mean displacement in the fracture. The resulting problem consists of equations of flow and mechanics in the fracture and the surrounding domain, accompanied by appropriate interface conditions.

2. We analyze the well-posedness of the DFM poroelasticity model using an iterative splitting technique, which provides explicit information about the convergence rate. The DFM model exhibits a similar parabolic-elliptic structure as the classical Biot system, enabling the use of monolithic methods such as in [38, 44]. However, our interest also extends to the numerical solution, where iterative splitting of flow and mechanics proves advantageous. The convergence of such splittings is a nontrivial issue that requires a careful analysis. Employing the optimized fixed-stress method [32], we prove the contractivity of the appropriate mapping, thereby demonstrating the well-posedness of the DFM poroelasticity. This result can later be used to design efficient numerical methods with a priori known convergence rate.

3. To demonstrate the application of the DFM model, we address a specific test problem involving the numerical solution of fluid injection into a fracture in a 2D setup. The study includes validation of the numerical results against an analytical solution and evaluation of robustness of the fixed-stress splitting method.

The structure of the paper is as follows. In section 2, we describe the full geometry with the classical Biot model and the reduced geometry containing the discrete fracture. Then, in section 3, we present the tangential and normal calculus, which will be used in the semi-discretization process in section 4. The process results in the DFM model (4.9) describing flow and mechanics in the matrix and in the fracture with appropriate interface conditions. In section 5, we analyze the existence and uniqueness of the solution to this problem, first studying the mechanics and flow equations separately and combining them later in the iterative scheme. Finally, in section 6, we describe the computational test problem, its discretization, and present the computed results.

2 Biot's poroelasticity in domain with fracture

Let Ω be a bounded, simply connected domain in the Euclidean space $\mathbf{R}^d$, $d \in \{2, 3\}$, with Lipschitz boundary $\partial\Omega$. We assume that Ω is composed of two subdomains: the matrix Ω_m and the fracture $\Omega_f := \Omega \setminus \overline{\Omega}_m$ that separates the matrix into two parts (see Figure 1).

We assume that the fracture domain has the form of a neighbourhood of a manifold; we consider hyperplane in $\mathbf{R}^d$ for the sake of simplicity. On the hyperplane with the unit normal $\boldsymbol{\nu}$, we consider a domain γ and the fracture

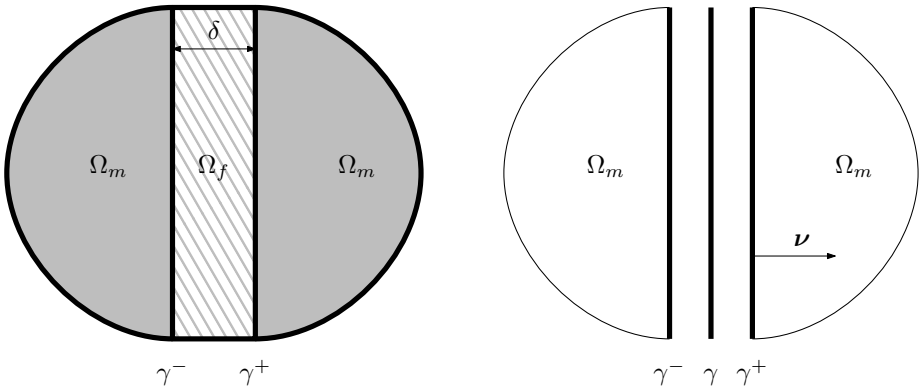

Figure 1: The domain of the full model (left) and the reduced geometry (right).

aperture $\delta > 0$, possibly dependent on $\mathbf{x}$, but independent of the displacement field. Then the fracture domain is assumed in the form:

$$\Omega_f = \{\mathbf{x} + s\boldsymbol{\nu};\ \mathbf{x} \in \gamma,\ s \in (-\tfrac{\delta}{2}, \tfrac{\delta}{2})\}.$$

The two parts of Ω_m are interacting with Ω_f via the interfaces

$$\gamma^+ := \{\mathbf{x} + \tfrac{\delta}{2}\boldsymbol{\nu};\ \mathbf{x} \in \gamma\}, \quad \gamma^- := \{\mathbf{x} - \tfrac{\delta}{2}\boldsymbol{\nu};\ \mathbf{x} \in \gamma\}.$$

The symbol $\partial\gamma$ shall denote the relative boundary of the domain γ with respect to the hyperplane. In the rest of this section, we shall describe the Biot system [5] on the domain Ω in the equivalent form of the separate equations in Ω_m and Ω_f coupled through the continuity conditions on the interfaces $\gamma^\pm$. The reduced system of equation on Ω_m and γ is derived later in section 4.

Let $I = (0, T)$ be a finite time interval. The balance of mass and forces in matrix and fracture is given by the equations

$$-\operatorname{div} \boldsymbol{\sigma} + \nabla(\alpha p) = \mathbf{f} \qquad \text{in } I \times (\Omega_m \cup \Omega_f), \tag{2.1a}$$

$$\partial_t \left(Sp + \operatorname{div}(\alpha \mathbf{u})\right) + \operatorname{div} \mathbf{q} = g \qquad \text{in } I \times (\Omega_m \cup \Omega_f). \tag{2.1b}$$

Here, the displacement $\mathbf{u}$ and the pressure p are the principal unknowns; further α is the Biot effective stress parameter, S the storativity, $\mathbf{f}$ the density of body force, and g the density of fluid source. The stress tensor $\boldsymbol{\sigma}$ and the flux $\mathbf{q}$ are determined by the Hooke and Darcy law, respectively:

$$\boldsymbol{\sigma} = \mathbb{C}\nabla\mathbf{u}, \quad \mathbf{q} = -\mathbb{K}\nabla p,$$

via the 4^{th}-order elasticity tensor $\mathbb{C}$ and the hydraulic conductivity tensor $\mathbb{K}$. We consider the initial condition for the given initial pressure p_0 and simple homogeneous Dirichlet boundary conditions:

$$p(0, \cdot) = p_0 \qquad \text{in } \Omega_m \cup \Omega_f, \tag{2.1c}$$

$$p = 0, \quad \mathbf{u} = \mathbf{0} \qquad \text{on } I \times \partial\Omega. \tag{2.1d}$$

To complete the system of equations, we have to specify interface conditions between matrix and fracture. To this end, we choose conditions equivalent to the piecewise heterogenous medium:

$$p, \mathbf{u}, \mathbf{q} \cdot \boldsymbol{\nu}, \boldsymbol{\sigma}\boldsymbol{\nu} - \alpha p \boldsymbol{\nu} \text{ are continuous on } I \times \gamma^\pm. \tag{2.1e}$$

In what follows, we shall assume that the physical parameters $\alpha, S, \mathbb{C}, \mathbb{K}$ are constant in Ω_m, Ω_f, respectively. To distinguish values in Ω_m and Ω_f, we shall use the subscripts "m" and "f", i.e. $\alpha_m := \alpha_{|\Omega_m}$, $\alpha_f := \alpha_{|\Omega_f}$ etc. We also impose standard requirements for the data:

- $\alpha_* \geq 0$, $S_* > 0$ for $* \in \{m, f\}$;
- $\mathbb{C}_*$ and $\mathbb{K}_*$, $* \in \{m, f\}$, have the usual symmetries:

$$\forall \mathbb{A}, \mathbb{B} \in \mathbf{R}^{d\times d}: \ \mathbb{C}_*\mathbb{A} : \mathbb{B} = \mathbb{C}_*\mathbb{A}^\top : \mathbb{B} = \mathbb{C}_*\mathbb{A} : \mathbb{B}^\top = \mathbb{C}_*\mathbb{B} : \mathbb{A},$$

$$\mathbb{K}_* = \mathbb{K}_*^\top;$$

- $\mathbb{C}_*$ and $\mathbb{K}_*$, $* \in \{m, f\}$, are positive definite: There exist positive constants μ_m, μ_f, λ_m, λ_f, κ_m, κ_f, such that

$$\forall \mathbb{A} \in \mathbf{R}^{d\times d}: \ \mathbb{C}_*\mathbb{A} : \mathbb{A} \geq \mu_* \left|\mathbb{A} + \mathbb{A}^\top\right|^2 + \lambda_* |\mathbb{I} : \mathbb{A}|^2, \tag{2.2}$$

$$\forall \mathbf{v} \in \mathbf{R}^d: \ \mathbb{K}_*\mathbf{v} \cdot \mathbf{v} \geq \kappa_* |\mathbf{v}|^2, \quad * \in \{m, f\}. \tag{2.3}$$

Here ":" stands for the scalar product in $\mathbf{R}^{d\times d}$ and $|\mathbb{A}|$ denotes the Frobenius norm, i.e. $|\mathbb{A}|^2 = \mathbb{A} : \mathbb{A}$.

In addition to the above assumptions on the data, we shall restrict ourselves to the case of highly permeable fracture, i.e.

$$|\mathbb{K}_m| \ll \kappa_f. \tag{2.4}$$

In such situations it is typical that pressure variations across the fracture are very small.

3 Preliminaries

In this section we introduce notation and tools that will be used later in the derivation of the DFM Biot model.

3.1 Tangential and normal calculus

Let $\mathbb{P} := \boldsymbol{\nu} \otimes \boldsymbol{\nu} = [\nu_i \nu_j]_{i,j=1}^d$ be the orthogonal projector to γ. For any vector $\mathbf{v} \in \mathbf{R}^d$ we introduce the orthogonal decomposition into normal and tangential direction to γ:

$$\mathbf{v} = \mathbf{v}_\nu + \mathbf{v}_\tau, \text{ where } \mathbf{v}_\nu := \mathbb{P}\mathbf{v} \text{ and } \mathbf{v}_\tau := (\mathbb{I} - \mathbb{P})\mathbf{v}.$$

The gradient operator of a function f, is decomposed into the normal and tangential part as follows:

$$\nabla f = (\nabla f)_\nu + (\nabla f)_\tau =: \nabla_\nu f + \nabla_\tau f.$$

We note that since the tangential gradient does not depend on values outside of γ, it is well-defined even for functions defined only in γ.

For vector- and tensor-valued functions we use analogous notation. In particular, tensors are decomposed to normal and tangential parts as follows:

$$\mathbb{A} = \mathbb{A}\mathbb{P} + \mathbb{A}(\mathbb{I} - \mathbb{P}) =: \mathbb{A}_\nu + \mathbb{A}_\tau.$$

Accordingly, we split the gradient of a vector-valued function:

$$\nabla \mathbf{v} = (\nabla \mathbf{v})_\nu + (\nabla \mathbf{v})_\tau =: \nabla_\nu \mathbf{v} + \nabla_\tau \mathbf{v}.$$

The divergence operators are decomposed as follows:

$$\begin{aligned}\operatorname{div} \mathbf{v} &= \operatorname{div} \mathbf{v}_\nu + \operatorname{div} \mathbf{v}_\tau =: \operatorname{div}_\nu \mathbf{v} + \operatorname{div}_\tau \mathbf{v},\\ \operatorname{div} \mathbb{A} &= \operatorname{div}(\mathbb{P}\mathbb{A}) + \operatorname{div}((\mathbb{I} - \mathbb{P})\mathbb{A}) =: \operatorname{div}_\nu \mathbb{A} + \operatorname{div}_\tau \mathbb{A}.\end{aligned}$$

We recall that the components of the Jacobian matrix and of the tensor divergence are given by $\nabla \mathbf{v} = \left[\frac{\partial v_i}{\partial x_j}\right]_{i,j=1}^{d}$ and $\operatorname{div} \mathbb{A} = \left[\sum_{j=1}^{d} \frac{\partial a_{ij}}{\partial x_j}\right]_{i=1}^{d}$, respectively.

Green's identity in γ reads:

$$\int_\gamma (\operatorname{div}_\tau \mathbf{v}) f = \int_{\partial\gamma} (\mathbf{v} \cdot \mathbf{n}) f - \int_\gamma \mathbf{v} \cdot \nabla_\tau f,$$

where $\mathbf{n}$ denotes the unit outward normal to $\partial\gamma$.

3.2 Averages, jumps and approximate gradients

The symbols $f^\oplus$ and $f^\ominus$ will denote the trace of f on γ^+, γ^-, respectively, i.e.

$$f^\oplus(\mathbf{x}) := f(\mathbf{x} \pm \tfrac{\delta}{2}\boldsymbol{\nu}),\ \mathbf{x} \in \gamma.$$

Using these symbols, we can introduce the average and jump operators:

$$\{\!\{f\}\!\} := \frac{f^\oplus + f^\ominus}{2}, \quad [\![f]\!] := f^\oplus - f^\ominus.$$

By $\overline{f}$ we shall denote the integral mean of f across the fracture aperture, i.e.

$$\overline{f}(\mathbf{x}) := \frac{1}{\delta} \int_{-\frac{\delta}{2}}^{\frac{\delta}{2}} f(\mathbf{x} + s\boldsymbol{\nu})\, \mathrm{d}s,\ \mathbf{x} \in \gamma.$$

For a pair of functions $f : \gamma^+ \cup \gamma^- \to \mathbf{R}$ and $F : \gamma \to \mathbf{R}$ we define the approximate gradient operator in the positive and negative half of fracture as follows:

$$\widetilde{\nabla}^\oplus(f, F) := \nabla_\tau F \pm \frac{2}{\delta}(f^\oplus - F)\boldsymbol{\nu}.$$

We also introduce the approximate gradient and divergence for vector-valued functions $\mathbf{v}, \mathbf{V}$:

$$\widetilde{\nabla}^\oplus(\mathbf{v}, \mathbf{V}) := \nabla_\tau \mathbf{V} \pm \frac{2}{\delta}(\mathbf{v}^\oplus - \mathbf{V}) \otimes \boldsymbol{\nu}, \quad \widetilde{\operatorname{div}}^\oplus(\mathbf{v}, \mathbf{V}) := \operatorname{div}_\tau \mathbf{V} \pm \frac{2}{\delta}(\mathbf{v}^\oplus - \mathbf{V}) \cdot \boldsymbol{\nu}.$$

3.3 Identities for averages and gradients

The integral means of differential operators satisfy the following relations:

$$\overline{\nabla f} = \nabla_\tau \overline{f} + \frac{1}{\delta} [\![f]\!] \boldsymbol{\nu} = \left\{\!\!\left\{ \widetilde{\nabla}(f, \overline{f}) \right\}\!\!\right\}, \tag{3.1}$$

$$\overline{\nabla \mathbf{v}} = \nabla_\tau \overline{\mathbf{v}} + \frac{1}{\delta} [\![\mathbf{v}]\!] \otimes \boldsymbol{\nu} = \left\{\!\!\left\{ \widetilde{\nabla}(\mathbf{v}, \overline{\mathbf{v}}) \right\}\!\!\right\}, \tag{3.2}$$

$$\overline{\operatorname{div} \mathbf{v}} = \operatorname{div}_\tau \overline{\mathbf{v}} + \frac{1}{\delta} [\![\mathbf{v}]\!] \cdot \boldsymbol{\nu} = \left\{\!\!\left\{ \widetilde{\operatorname{div}}(\mathbf{v}, \overline{\mathbf{v}}) \right\}\!\!\right\}, \tag{3.3}$$

$$\overline{\operatorname{div} \mathbb{A}} = \operatorname{div}_\tau \overline{\mathbb{A}} + \frac{1}{\delta} [\![\mathbb{A}^\top]\!] \boldsymbol{\nu}. \tag{3.4}$$

For the proof, we refer to Appendix A.

Furthermore, for twice continuously differentiable functions $f \in \mathcal{C}^2(\overline{\Omega}_f)$, Taylor's expansion implies that

$$f^\oplus = \overline{f} + O(\delta), \quad (\nabla f)^\oplus = \widetilde{\nabla}^\oplus(f, \overline{f}) + O(\delta). \tag{3.5}$$

Here the remainder $O(\delta)$ represents an expression that can be estimated from above by $\delta C \|f\|_{\mathcal{C}^2(\overline{\Omega}_f)}$ where $C > 0$ is independent of f and δ.

4 Semi-discretization process

Let us assume that $(\mathbf{u}, p)$ is a smooth solution of (2.1). We shall use the calculus from section 3 to derive appropriate equations that are satisfied by the averages $(\overline{\mathbf{u}}, \overline{p})$ in $I \times \gamma$.

4.1 Fracture model for elasticity

Integrating (2.1a) over the fracture aperture yields:

$$-\delta \overline{\operatorname{div} \sigma} + \delta \alpha_f \overline{\nabla p} = \delta \overline{\mathbf{f}} \text{ in } I \times \gamma.$$

To express the averaged terms on the left-hand side we use (3.4), (3.2) and (3.1). In particular, we obtain:

$$\overline{\operatorname{div} \sigma} = \operatorname{div}_\tau \left(\mathbb{C}_f \left\{\!\!\left\{ \widetilde{\nabla}(\mathbf{u}, \overline{\mathbf{u}}) \right\}\!\!\right\} \right) + \frac{1}{\delta} [\![\mathbb{C}_f \nabla \mathbf{u}_{|\Omega_f}]\!] \boldsymbol{\nu}.$$

The normal stress $(\mathbb{C}_f \nabla \mathbf{u}_{|\Omega_f})^\oplus \boldsymbol{\nu}$ will be approximated by the quantity

$$\mathbf{t}^\oplus(\mathbf{u}, \overline{\mathbf{u}}) := \left(\mathbb{C}_f \widetilde{\nabla}^\oplus(\mathbf{u}, \overline{\mathbf{u}}) \right) \boldsymbol{\nu} \tag{4.1}$$

with an error of $O(\delta^2)$. Altogether, we get the reduced counterpart of (2.1a):

$$-\delta \operatorname{div}_\tau \left(\mathbb{C}_f \left\{\!\!\left\{ \widetilde{\nabla}(\mathbf{u}, \overline{\mathbf{u}}) \right\}\!\!\right\} \right) + \delta \alpha_f \overline{\nabla p} - [\![\mathbf{t}(\mathbf{u}, \overline{\mathbf{u}})]\!] = \delta \overline{\mathbf{f}} + O(\delta) \text{ in } I \times \gamma. \tag{4.2}$$

In accordance with the assumption of permeable fracture (2.4) we assume that $\nabla_\nu p$ is negligible, so that

$$p^\oplus = \overline{p} + O(\delta) \text{ and } \overline{\nabla p} = \nabla_\tau \overline{p} + O(\delta).$$

Then, taking into account (3.5), we obtain from (4.2):

$$-\delta \operatorname{div}_\tau \left(\mathbb{C}_f \left\{\!\!\left\{ \widetilde{\nabla}(\mathbf{u}, \overline{\mathbf{u}}) \right\}\!\!\right\} \right) + \delta \alpha_f \nabla_\tau \overline{p} - [\![\mathbf{t}(\mathbf{u}, \overline{\mathbf{u}})]\!] = \delta \overline{\mathbf{f}} + O(\delta) \text{ in } I \times \gamma. \quad (4.3)$$

The continuity of normal poroelastic stress $\varpi \boldsymbol{\nu} - \alpha p \boldsymbol{\nu}$ on $\gamma^\pm$ becomes

$$(\mathbb{C}_m (\nabla \mathbf{u}_{|\Omega_m})^\oplus - \alpha_m p^\oplus \mathbb{I}) \boldsymbol{\nu} = \mathbf{t}^\oplus(\mathbf{u}, \overline{\mathbf{u}}) - \alpha_f \overline{p} \boldsymbol{\nu} + O(\delta) \text{ in } I \times \gamma. \quad (4.4)$$

4.2 Fracture model for flow

Let us integrate (2.1b) over the fracture aperture. We get:

$$\partial_t \left(\delta S_f \overline{p} + \delta \alpha_f \overline{\operatorname{div} \mathbf{u}} \right) + \delta \overline{\operatorname{div} \mathbf{q}} = \delta \overline{g} \text{ in } I \times \gamma. \quad (4.5)$$

From (3.3), (3.1) and the definition of $\mathbf{q}$ we obtain:

$$\overline{\operatorname{div} \mathbf{q}} = \operatorname{div}_\tau \overline{\mathbf{q}} + \frac{1}{\delta} [\![\mathbf{q}]\!] \cdot \boldsymbol{\nu} = -\operatorname{div}_\tau \left(\mathbb{K}_f \left\{\!\!\left\{ \widetilde{\nabla}[p, \overline{p}] \right\}\!\!\right\} \right) + \frac{1}{\delta} [\![\mathbf{q}]\!] \cdot \boldsymbol{\nu}.$$

To express the approximation of the normal flux $-\mathbf{q}^\oplus \cdot \boldsymbol{\nu}$ we use the quantity

$$\varphi^\oplus(p, \overline{p}) := \mathbb{K}_f \widetilde{\nabla}^\oplus(p, \overline{p}) \cdot \boldsymbol{\nu}. \quad (4.6)$$

Hence, we obtain from (4.5)–(4.6) and (3.3) the reduced flow equation:

$$\delta \partial_t \left(S_f \overline{p} + \alpha_f \left\{\!\!\left\{ \widetilde{\operatorname{div}}[\mathbf{u}, \overline{\mathbf{u}}] \right\}\!\!\right\} \right) - \delta \operatorname{div}_\tau \left(\mathbb{K}_f \left\{\!\!\left\{ \widetilde{\nabla}(p, \overline{p}) \right\}\!\!\right\} \right) - [\![\varphi(p, \overline{p})]\!] = \delta \overline{g} + O(\delta) \text{ in } I \times \gamma. \quad (4.7)$$

The continuity of the flux through $\gamma^\pm$ yields:

$$\mathbb{K}_m (\nabla p_{|\Omega_m})^\oplus \cdot \boldsymbol{\nu} = \varphi^\oplus(p, \overline{p}) + O(\delta) \text{ in } I \times \gamma. \quad (4.8)$$

4.3 DFM model of poroelasticity

The coupled DFM model is obtained after neglecting the remainders $O(\delta)$ in (4.3), (4.4), (4.7), (4.8). Analysis of the truncation error can be done similarly as in [13], however in this paper we omit it. Let $\Gamma := \partial\Omega_m \cap \partial\Omega$, $P_0 = (P_{0m}, P_{0f}) := (p_{0|\Omega_m}, \overline{p}_0)$, $\mathbf{F} = (\mathbf{F}_m, \mathbf{F}_f) := (\mathbf{f}_{|\Omega_m}, \delta \overline{\mathbf{f}})$ and $G = (G_m, G_f) := (g_{|\Omega_m}, \delta \overline{g})$. We want to find functions $\mathbf{U} = (\mathbf{U}_m, \mathbf{U}_f)$ and $P = (P_m, P_f)$, where $\mathbf{U}_m, P_m$ are defined in $I \times \Omega_m$ and $\mathbf{U}_f, P_f$ are defined in $I \times \gamma$, which satisfy:

(i) Biot's equations for the matrix:

$$-\operatorname{div}(\mathbb{C}_m \nabla \mathbf{U}_m) + \alpha_m \nabla P_m = \mathbf{F}_m \quad \text{in } I \times \Omega_m, \quad (4.9a)$$

$$\partial_t (S_m P_m + \alpha_m \operatorname{div} \mathbf{U}_m) - \operatorname{div}(\mathbb{K}_m \nabla P_m) = G_m \quad \text{in } I \times \Omega_m, \quad (4.9b)$$

(ii) averaged Biot's equations for the fracture:

$$-\delta \operatorname{div}_\tau \left(\mathbb{C}_f \left\{\!\!\left\{ \widetilde{\nabla} \mathbf{U} \right\}\!\!\right\} \right) + \delta \alpha_f \nabla_\tau P_f - [\![\mathbf{t}(\mathbf{U})]\!] = \mathbf{F}_f \text{ in } I \times \gamma, \quad (4.9c)$$

$$\delta \partial_t \left(S_f P_f + \alpha_f \left\{\!\!\left\{ \widetilde{\operatorname{div}} \mathbf{U} \right\}\!\!\right\} \right) - \delta \operatorname{div}_\tau \left(\mathbb{K}_f \left\{\!\!\left\{ \widetilde{\nabla} P \right\}\!\!\right\} \right) - [\![\varphi(P)]\!] = G_f \text{ in } I \times \gamma, \quad (4.9d)$$

(iii) interface conditions:

$$(\mathbb{C}_m(\nabla \mathbf{U}_m)^{\oplus} - \alpha_m P_m^{\oplus}\mathbb{I})\boldsymbol{\nu} = \mathbf{t}^{\oplus}(\mathbf{U}) - \alpha_f P_f \boldsymbol{\nu} \qquad \text{in } I \times \gamma, \tag{4.9e}$$

$$\mathbb{K}_m(\nabla P_m)^{\oplus} \cdot \boldsymbol{\nu} = \varphi^{\oplus}(P) \qquad \text{in } I \times \gamma, \tag{4.9f}$$

(iv) boundary and initial conditions:

$$\mathbf{U} = \mathbf{0}, \quad P = 0 \qquad \text{on } I \times (\Gamma \times \partial\gamma), \tag{4.9g}$$

$$P(0,\cdot) = P_0 \qquad \text{in } \Omega_m \times \gamma. \tag{4.9h}$$

We point out that $\mathbf{U}_f$ and P_f play the role of approximations of the averages $\overline{\mathbf{u}}$ and $\overline{p}$ in Ω_f.

Remark 4.1. *In [9], another DFM model of linearized poroelasticity was obtained using a different approach (see problem (4.11) therein). That model was derived from a mixed-dimensional version of continuum-mechanics laws, postulated directly in a domain containing the reduced geometry of fractures. This makes the resulting model less obvious to compare with our model (4.9) obtained by semi-discretization. The poroelastic coupling terms used in [9] are defined in terms of mixed-dimensional operators, namely the symmetric gradient $\mathfrak{D}_s$ and the co-symmetric gradient $\mathbb{D}_s\cdot$, which are by definition mutually adjoint. This enables to retain the integration by parts formula, necessary for obtaining the energy estimate. In contrast, our operators $\widetilde{\nabla}$ and $\widetilde{\mathrm{div}}$, which naturally appear as the result of semi-discretization, do not satisfy the integration by parts, therefore the additional hypothesis (2.4) of permeable fracture is required to obtain a mathematically well-posed problem. Another point of difference between [9] and the present paper stems from the use of different measures of volumetric change (cf. the quantity $\left\{\!\left\{\widetilde{\mathrm{div}}\mathbf{U}\right\}\!\right\}$ in our paper with $\mathfrak{T}'(\mathfrak{e})$ and Example 3.6 in [9]).*

5 Well-posedness

In this section, we first introduce the weak formulation of (4.9). Then we analyze separately the mechanical and the flow part of the problem. Finally, we combine both subproblems in the fixed-stress iterative process and prove its convergence to the solution of the coupled problem.

In what follows, we shall use the symbols $L^2(D;Y)$, $H^1(D;Y)$ for the Lebesgue and Sobolev spaces of functions defined in D and taking values in Y. If $Y = \mathbf{R}$, then we shall write simply $L^2(D)$, $H^1(D)$. Further, $H^1_0(D;Y)$ and $H^1_B(D;Y)$ will be the subspaces of $H^1(D;Y)$ for the functions vanishing on the boundary and on a part of the boundary B, respectively. The symbol $L^2(I;X)$ will denote the Bochner space and $H^1(I;X)$ its subspace of functions with a time derivative in $L^2(I;X)$. By $\langle y, x\rangle_X$ we shall denote the duality pairing between a Banach space X and its dual X^*, with $x \in X$ and $y \in X^*$.

For the weak formulation, we introduce the spaces

$$\boldsymbol{\mathcal{V}} := H^1_\Gamma(\Omega_m;\mathbf{R}^d) \times H^1_0(\gamma;\mathbf{R}^d),$$

$$\mathscr{L} := L^2(\Omega_m) \times L^2(\gamma),$$

$$\mathcal{V} := H^1_\Gamma(\Omega_m) \times H^1_0(\gamma).$$

If $\mathbf{V} \in \boldsymbol{\mathcal{V}}$, then its components will be denoted $\mathbf{V}_m$ and $\mathbf{V}_f$ that is, $\mathbf{V} := (\mathbf{V}_m, \mathbf{V}_f)$. The same notation will be used for elements of $\mathscr{L}$ and $\mathcal{V}$. The above spaces are equipped by the following norms:

$$\|\mathbf{V}\|_{\boldsymbol{\mathcal{V}}} := (\|\nabla \mathbf{V}_m\|^2_{L^2(\Omega_m)} + \|\nabla_\tau \mathbf{V}_f\|^2_{L^2(\gamma)})^{1/2},$$
$$\|Q\|_{\mathscr{L}} := (\|Q_m\|^2_{L^2(\Omega_m)} + \|Q_f\|^2_{L^2(\gamma)})^{1/2},$$
$$\|Q\|_{\mathcal{V}} := (\|\nabla Q_m\|^2_{L^2(\Omega_m)} + \|\nabla_\tau Q_f\|^2_{L^2(\gamma)})^{1/2}.$$

For a proper functional setting of the weak formulation, we first show the a priori estimate of the solution to (4.9). Namely, formal calculations (see appendix B) lead to the following "energy equality":

$$\int_{\Omega_m} \mathbb{C}_m \nabla \partial_t \mathbf{U}_m : \nabla \partial_t \mathbf{U}_m + \delta \int_\gamma \left\{\!\!\left\{ \mathbb{C}_f \widetilde{\nabla} \partial_t \mathbf{U} : \widetilde{\nabla} \partial_t \mathbf{U} \right\}\!\!\right\}$$
$$+ S_m \int_{\Omega_m} |\partial_t P_m|^2 + \delta S_f \int_\gamma |\partial_t P_f|^2 + \frac{1}{2}\frac{\mathrm{d}}{\mathrm{d}t} \int_{\Omega_m} \mathbb{K}_m \nabla P_m \cdot \nabla P_m + \frac{\delta}{2}\frac{\mathrm{d}}{\mathrm{d}t} \int_\gamma \left\{\!\!\left\{ \mathbb{K}_f \widetilde{\nabla} P \cdot \widetilde{\nabla} P \right\}\!\!\right\}$$
$$= \langle \partial_t \mathbf{F}, \partial_t \mathbf{U}_m \rangle_{\boldsymbol{\mathcal{V}}} + \langle G, \partial_t P_m \rangle_{\mathcal{V}}\,. \quad (5.1)$$

The identity yields a priori bounds of the solution:

$$\partial_t \mathbf{U} \in L^2(I; \boldsymbol{\mathcal{V}}), \quad P \in L^\infty(I; \mathcal{V}), \quad \partial_t P \in L^2(I; \mathscr{L})$$

provided that the data are sufficiently smooth. We therefore introduce another function space:

$$\mathcal{X} := L^\infty(I; \mathcal{V}) \cap H^1(I; \mathscr{L})$$

to which the pressure P should belong. The weak formulation of (4.9) reads (see Appendix B for the derivation):

Find $\mathbf{U} \in H^1(I; \boldsymbol{\mathcal{V}})$ *and* $P \in \mathcal{X}$ *such that*

$$P(0, \cdot) = P_0; \quad (5.2a)$$

for all $\mathbf{V} \in \boldsymbol{\mathcal{V}}$ *and a.a.* $t \in I$*:*

$$\int_{\Omega_m} (\mathbb{C}_m \nabla \mathbf{U}_m : \nabla \mathbf{V}_m - \alpha_m P_m \operatorname{div} \mathbf{V}_m) + \delta \int_\gamma \left\{\!\!\left\{ \mathbb{C}_f \widetilde{\nabla} \mathbf{U} : \widetilde{\nabla} \mathbf{V} - \alpha_f P_f \widetilde{\operatorname{div}} \mathbf{V} \right\}\!\!\right\}$$
$$= \langle \mathbf{F}, \mathbf{V} \rangle_{\boldsymbol{\mathcal{V}}}\,; \quad (5.2b)$$

for all $Q \in \mathcal{V}$ *and a.a.* $t \in I$*:*

$$\int_{\Omega_m} (Q_m \partial_t (S_m P_m + \alpha_m \operatorname{div} \mathbf{U}_m) + \mathbb{K}_m \nabla P_m \cdot \nabla Q_m) + \delta \int_\gamma Q_f \partial_t \left(S_f P_f + \alpha_f \left\{\!\!\left\{ \widetilde{\operatorname{div}} \mathbf{U} \right\}\!\!\right\} \right)$$
$$+ \delta \int_\gamma \left\{\!\!\left\{ \mathbb{K}_f \widetilde{\nabla} P \cdot \widetilde{\nabla} Q \right\}\!\!\right\} = \langle G, Q \rangle_{\mathscr{L}}\,. \quad (5.2c)$$

We state the main result of the paper.

Theorem 5.1. *Let* $\mathbf{F} \in H^1(I; \boldsymbol{\mathcal{V}}^*)$*,* $G \in L^2(I; \mathscr{L})$*, and* $P_0 \in \mathcal{V}$*. Then* (5.2) *has a unique solution.*

The proof will be done in several steps. First, we solve separately the mechanical and flow subproblem, respectively. Then we define a suitable iterative scheme alternating between the subproblems, which will be shown to be convergent.

5.1 Mechanical subproblem

In this section, we consider only the mechanical part of the problem (5.2). Assuming that P is a given pressure field at some time $t \in I$, we define the following forms in $\boldsymbol{\mathcal{V}}$:

$$a(\mathbf{U},\mathbf{V}) := \int_{\Omega_m} \mathbb{C}_m \nabla \mathbf{U}_m : \nabla \mathbf{V}_m + \delta \int_\gamma \left\{\!\!\left\{ \mathbb{C}_f \widetilde{\nabla} \mathbf{U} : \widetilde{\nabla} \mathbf{V} \right\}\!\!\right\},$$

$$l(\mathbf{V}) := \langle \mathbf{F}, \mathbf{V} \rangle_{\boldsymbol{\mathcal{V}}} + \int_{\Omega_m} \alpha_m P_m \operatorname{div} \mathbf{V}_m + \delta \int_\gamma \alpha_f P_f \left\{\!\!\left\{ \widetilde{\operatorname{div}} \mathbf{V} \right\}\!\!\right\}.$$

Then we introduce the problem:

$$\text{Find } \mathbf{U} \in \boldsymbol{\mathcal{V}} \text{ such that for all } \mathbf{V} \in \boldsymbol{\mathcal{V}}\text{: } a(\mathbf{U},\mathbf{V}) = l(\mathbf{V}). \tag{5.3}$$

The existence and uniqueness of the solution to (5.3) will be proved using the Lax-Milgram theorem. To ensure ellipticity of the bilinear form a, we first prove a suitable inequality for the functions in $\boldsymbol{\mathcal{V}}$.

Korn type inequalities. Let us recall the classical Korn inequality: For any bounded domain $D \subset \mathbf{R}^d$ with Lipschitz boundary and a nontrivial part $B \subset \partial D$ there is a constant $C_K := C_K(D,B) > 0$ such that

$$\forall \mathbf{v} \in H^1_B(D;\mathbf{R}^d) : \; C_K \left\|\nabla \mathbf{v}\right\|_{L^2(D)} \le \left\|\boldsymbol{\varepsilon}(\mathbf{v})\right\|_{L^2(D)}, \tag{5.4}$$

where $\boldsymbol{\varepsilon}(\mathbf{v}) := \frac{1}{2}(\nabla \mathbf{v} + (\nabla \mathbf{v})^\top)$. For any function $\mathbf{V}_f \in H^1(\gamma;\mathbf{R}^d)$, we denote its symmetrized tangential gradient by

$$\boldsymbol{\varepsilon}_\tau(\mathbf{V}_f) := \frac{1}{2}(\nabla_\tau \mathbf{V}_f + (\nabla_\tau \mathbf{V}_f)^\top).$$

Similarly for $\mathbf{V} \in \boldsymbol{\mathcal{V}}$ we define its symmetrized approximate gradient by

$$\tilde{\boldsymbol{\varepsilon}}^{\oplus}(\mathbf{V}) := \frac{1}{2}(\widetilde{\nabla}^{\oplus} \mathbf{V} + (\widetilde{\nabla}^{\oplus} \mathbf{V})^\top).$$

We have the following Korn inequality in $H^1_0(\gamma)$.

Lemma 5.2. *There exists a constant $C_1 > 0$ such that for all $\mathbf{V}_f \in H^1_0(\gamma;\mathbf{R}^d)$ it holds:*

$$C_1 \left\|\nabla_\tau \mathbf{V}_f\right\|^2_{L^2(\gamma)} \le \left\|\boldsymbol{\varepsilon}_\tau(\mathbf{V}_f)\right\|^2_{L^2(\gamma)}. \tag{5.5}$$

Proof. Let $\mathbf{V}_f \in H^1_0(\gamma;\mathbf{R}^d)$. From the definition of the tangential operators it follows that

$$\left\|\boldsymbol{\varepsilon}_\tau(\mathbf{V}_{f\nu})\right\|^2_{L^2(\gamma)} = \tfrac{1}{2} \left\|\nabla_\tau \mathbf{V}_{f\nu}\right\|^2_{L^2(\gamma)},$$

which implies

$$\left\|\boldsymbol{\varepsilon}_\tau(\mathbf{V}_f)\right\|^2_{L^2(\gamma)} = \left\|\boldsymbol{\varepsilon}_\tau(\mathbf{V}_{f\tau})\right\|^2_{L^2(\gamma)} + \tfrac{1}{2} \left\|\nabla_\tau \mathbf{V}_{f\nu}\right\|^2_{L^2(\gamma)}.$$

Further, by mapping $\mathbf{V}_f$ isometrically from γ to a subset of $\mathbf{R}^{d-1}$, we can apply (5.4) to the tangential part $\mathbf{V}_{f\tau}$, which implies:

$$\left\|\boldsymbol{\varepsilon}_\tau(\mathbf{V}_{f\tau})\right\|^2_{L^2(\gamma)} \ge C_K \left\|\nabla_\tau \mathbf{V}_{f\tau}\right\|^2_{L^2(\gamma)}.$$

Altogether we have:

$$\|\boldsymbol{\varepsilon}_\tau(\mathbf{V}_f)\|^2_{L^2(\gamma)} \geq \min\{C_K, \tfrac{1}{2}\} \|\nabla_\tau \mathbf{V}_f\|^2_{L^2(\gamma)},$$

which proves (5.5). □

Now we can prove a variant of the Korn inequality in $\boldsymbol{\mathcal{V}}$, which takes into account the approximate gradient.

Lemma 5.3. *There exists a constant $C_2 > 0$ such that for all $\mathbf{V} \in \boldsymbol{\mathcal{V}}$ it holds:*

$$C_2 \|\mathbf{V}\|^2_{\boldsymbol{\mathcal{V}}} \leq \|\boldsymbol{\varepsilon}(\mathbf{V}_m)\|^2_{L^2(\Omega_m)} + \left\{\!\!\left\{ \|\tilde{\boldsymbol{\varepsilon}}(\mathbf{V})\|^2_{L^2(\gamma)} \right\}\!\!\right\}. \tag{5.6}$$

Proof. Let us assume for contradiction that there is a sequence $\{\mathbf{V}^n\}_{n=1}^\infty$ in $\boldsymbol{\mathcal{V}}$ such that

$$\|\boldsymbol{\varepsilon}(\mathbf{V}^n_m)\|^2_{L^2(\Omega_m)} + \left\{\!\!\left\{ \|\tilde{\boldsymbol{\varepsilon}}(\mathbf{V}^n)\|^2_{L^2(\gamma)} \right\}\!\!\right\} < \frac{1}{n} \|\mathbf{V}^n\|^2_{\boldsymbol{\mathcal{V}}}. \tag{5.7}$$

Without loss of generality we may assume that $\|\mathbf{V}^n\|_{\boldsymbol{\mathcal{V}}} = 1$, so that

$$\mathbf{V}^n \rightharpoonup \mathbf{V} \text{ weakly in } \boldsymbol{\mathcal{V}},\ n \to \infty, \tag{5.8}$$

where $\mathbf{V} \in \boldsymbol{\mathcal{V}}$, passing eventually to a subsequence. From (5.7) and the Korn inequality in $H^1_\Gamma(\Omega_m; \mathbf{R}^d)$ it follows that

$$\mathbf{V}^n_m \to \mathbf{0} \text{ strongly in } H^1_\Gamma(\Omega_m; \mathbf{R}^d),\ n \to \infty, \tag{5.9}$$

implying that $\mathbf{V}_m = \mathbf{0}$. From (5.7) it also follows that

$$\tilde{\boldsymbol{\varepsilon}}^{\oplus}(\mathbf{V}^n) \to 0 \text{ strongly in } L^2(\gamma; \mathbf{R}^{d\times d}),\ n \to \infty. \tag{5.10}$$

Using this together with the definition of $\tilde{\boldsymbol{\varepsilon}}^{\oplus}$, (5.8), (5.9) and the embedding $H^1(\Omega_m) \hookrightarrow L^2(\gamma)$, we obtain:

$$\boldsymbol{\varepsilon}_\tau(\mathbf{V}_f) = \pm\frac{1}{\delta}(\mathbf{V}_f \otimes \boldsymbol{\nu} + \boldsymbol{\nu} \otimes \mathbf{V}_f),$$

from which it follows that $\mathbf{V}_f \otimes \boldsymbol{\nu} + \boldsymbol{\nu} \otimes \mathbf{V}_f = \mathbb{0}$ and thus $\mathbf{V}_f = \mathbf{0}$.

With help of the compact embedding $H^1(\gamma) \hookrightarrow L^2(\gamma)$ we deduce from (5.10) that $\boldsymbol{\varepsilon}_\tau(\mathbf{V}^n_f) \to \mathbb{0}$ strongly in $L^2(\gamma; \mathbf{R}^{d\times d})$, $n \to \infty$. Lemma 5.2 then implies that also $\mathbf{V}^n_f \to \mathbf{0}$ strongly in $H^1_0(\gamma; \mathbf{R}^d)$, $n \to \infty$. Finally, having shown the strong convergence of $\{\mathbf{V}^n\}_{n=1}^\infty$, we observe that

$$1 = \lim_{n\to\infty} \|\mathbf{V}^n\|_{\boldsymbol{\mathcal{V}}} = \|\mathbf{V}\|_{\boldsymbol{\mathcal{V}}} = 0,$$

which is a contradiction. Therefore, the proof is finished. □

Existence and uniqueness of solutions. In the following lemma, we prove several important properties of a and l.

Lemma 5.4. *The bilinear form a is bounded and elliptic in $\boldsymbol{\mathcal{V}}$ and the linear form l is bounded in $\boldsymbol{\mathcal{V}}$. In particular, there exist constants $C_3 = C_3(C_2, \delta, \mu_m, \mu_f) > 0$ and $C_4 = C_4(\alpha_m, \alpha_f, \delta, \gamma^+, \gamma^-, \Omega_m) > 0$ such that*

$$a(\mathbf{V}, \mathbf{V}) \geq C_3 \|\mathbf{V}\|^2_{\boldsymbol{\mathcal{V}}},$$

$$l(\mathbf{V}) \leq (\|\mathbf{F}\|_{\boldsymbol{\mathcal{V}}^*} + C_4 \|P\|_{\mathscr{L}}) \|\mathbf{V}\|_{\boldsymbol{\mathcal{V}}}$$

for all $\mathbf{V} \in \boldsymbol{\mathcal{V}}$.

Proof. The boundedness of a and l is a straightforward consequence of embeddings $H^1(\Omega_m) \hookrightarrow L^2(\gamma^\pm)$ and standard inequalities; we prove only the ellipticity. For any $\mathbf{V} \in \boldsymbol{\mathcal{V}}$ we have:

$$a(\mathbf{V},\mathbf{V}) = \int_{\Omega_m} \mathbb{C}_m \nabla \mathbf{V}_m : \nabla \mathbf{V}_m + \delta \int_\gamma \left\{\!\!\left\{ \mathbb{C}_f \widetilde{\nabla} \mathbf{V} : \widetilde{\nabla} \mathbf{V} \right\}\!\!\right\}.$$

Now we can apply (2.2) and (5.6), which yields:

$$a(\mathbf{V},\mathbf{V}) \geq 2\mu_m \left\|\boldsymbol{\varepsilon}(\mathbf{V}_m)\right\|^2_{L^2(\Omega_m)} + 2\mu_f \delta \left\{\!\!\left\{ \left\|\widetilde{\boldsymbol{\varepsilon}}(\mathbf{V})\right\|^2_{L^2(\gamma)} \right\}\!\!\right\}$$
$$\geq 2C_2 \min\{\mu_m, \mu_f\delta\} \left\|\mathbf{V}\right\|^2_{\boldsymbol{\mathcal{V}}}.$$

From this we see that a is elliptic with the constant $C_3 = 2C_2 \min\{\mu_m, \mu_f\delta\}$. □

Having shown the above properties of the forms a and l, the following result is a direct consequence of the Lax-Milgram theorem.

Theorem 5.5. *Let $\mathbf{F} \in \boldsymbol{\mathcal{V}}^*$ and $P \in \mathscr{L}$. Then problem (5.3) has a unique solution $\mathbf{U} \in \boldsymbol{\mathcal{V}}$ which satisfies:*

$$\left\|\mathbf{U}\right\|_{\boldsymbol{\mathcal{V}}} \leq \frac{1}{C_3}\Big(\left\|\mathbf{F}\right\|_{\boldsymbol{\mathcal{V}}^*} + C_4 \left\|P\right\|_{\mathscr{L}} \Big).$$

Now, we consider the time-dependent case. If $(\mathbf{F}_m, \mathbf{F}_f, P_m, P_f)$ are defined in the time interval I, then by differentiating the identity in (5.3) with respect to time we observe that $\partial_t \mathbf{U}$ satisfies for all $\mathbf{V} \in \boldsymbol{\mathcal{V}}$:

$$a(\partial_t \mathbf{U}, \mathbf{V}) = l_t(\mathbf{V}), \tag{5.11}$$

where l_t stands for the linear form

$$l_t(\mathbf{V}) := \langle \partial_t \mathbf{F}, \mathbf{V} \rangle_{\boldsymbol{\mathcal{V}}} + \int_{\Omega_m} \alpha_m \partial_t P_m \operatorname{div} \mathbf{V}_m + \delta \int_\gamma \alpha_f \partial_t P_f \left\{\!\!\left\{ \widetilde{\operatorname{div}} \mathbf{V} \right\}\!\!\right\}.$$

Similarly as in Lemma 5.4, one can show that l_t is bounded and estimate it in terms of the time derivatives of the data:

$$l_t(\mathbf{V}) \leq \left(\left\|\partial_t \mathbf{F}\right\|_{\boldsymbol{\mathcal{V}}^*} + C_4 \left\|\partial_t P\right\|_{\mathscr{L}}\right) \left\|\mathbf{V}\right\|_{\boldsymbol{\mathcal{V}}}.$$

Since the solution mappings $(\mathbf{F}, P) \mapsto \mathbf{U}$ and $(\partial_t \mathbf{F}, \partial_t P) \mapsto \partial_t \mathbf{U}$ are linear and bounded, we obtain:

Corollary 5.6. *Let $\mathbf{F} \in L^2(I; \boldsymbol{\mathcal{V}}^*)$ and $P \in L^2(I; \mathscr{L})$. Denoting by $\mathbf{U}[t]$ the solution to (5.3) with the data $\mathbf{F}[t], P[t]$, we have $\mathbf{U} \in L^2(I; \boldsymbol{\mathcal{V}})$. If in addition $\partial_t \mathbf{F} \in L^2(I; \boldsymbol{\mathcal{V}}^*)$ and $\partial_t P \in L^2(I; \mathscr{L})$, then also $\partial_t \mathbf{U} \in L^2(I; \boldsymbol{\mathcal{V}})$.*

Based on the above result, we define the mapping $\mathcal{E} : H^1(I; \mathscr{L}) \to H^1(I; \boldsymbol{\mathcal{V}})$ by the relation

$$\mathcal{E}(P)[t] := \mathbf{U}[t].$$

We shall use it in the definition of the fixed-stress splitting in section 5.3.

5.2 Flow subproblem

We now turn to the flow part of the DFM model (5.2), assuming zero displacements. We want to solve the following problem:

Find $P \in \mathcal{X}$ such that

$$P(0,\cdot) = P_0; \tag{5.12a}$$

and for all $Q \in \mathcal{V}$ and a.a. $t \in I$:

$$\int_{\Omega_m} (S_m Q_m \partial_t P_m + \mathbb{K}_m \nabla P_m \cdot \nabla Q_m) + \delta S_f \int_\gamma Q_f \partial_t P_f + \delta \int_\gamma \left\{\!\!\left\{ \mathbb{K}_f \widetilde{\nabla} P \cdot \widetilde{\nabla} Q \right\}\!\!\right\} = \left\langle \tilde{G}, Q \right\rangle_{\mathscr{L}}. \tag{5.12b}$$

Here $\tilde{G} := (\tilde{G}_m, \tilde{G}_f)$ are modified fluid sources to be specified in section 5.3. The well-posedness of (5.12) will be established on the base of standard theory of parabolic problems (see e.g., [16], chap. 7.1). We formulate the result in the following theorem.

Theorem 5.7. *Let $P_0 \in \mathcal{V}$ and $\tilde{G} \in L^2(I;\mathscr{L})$. Then there exists a unique solution to (5.12).*

Proof. Existence: Let $\{w_j\}_{j=1}^\infty$ and $\{W_j\}_{j=1}^\infty$ be bases in $H^1_\Gamma(\Omega_m)$, $H^1_0(\gamma)$, respectively, orthonormal with respect to the L^2-scalar products. For any $n = 1, 2, ...$ we define the Galerkin approximation $P^n := (P^n_m, P^n_f)$ in the form $P^n_m(t,\mathbf{x}) := \sum_{j=1}^n \psi^n_j(t) w_j(\mathbf{x})$, $P^n_f(t,\mathbf{x}) := \sum_{j=1}^n \Psi^n_j(t) W_j(\mathbf{x})$, satisfying for a.a. $t \in I$ and for $i = 1, ..., n$ the integral identities

$$S_m \int_{\Omega_m} w_i \partial_t P_{nm} + \int_{\Omega_m} \mathbb{K}_m \nabla P^n_m \cdot \nabla w_i + \delta \int_\gamma \left\{\!\!\left\{ \mathbb{K}_f \widetilde{\nabla} P^n \cdot \widetilde{\nabla}[w_i, 0] \right\}\!\!\right\} + \int_\gamma [\![\varphi(P^n) w_i]\!] = \int_{\Omega_m} \tilde{G}_m w_i, \tag{5.13}$$

$$\delta S_f \int_\gamma W_i \partial_t P_{nf} + \delta \int_\gamma \mathbb{K}_f \left\{\!\!\left\{ \widetilde{\nabla} P^n \right\}\!\!\right\} \cdot \nabla_\tau W_i - \int_\gamma [\![\varphi(P^n) W_i]\!] = \int_\gamma \tilde{G}_f W_i, \tag{5.14}$$

and the initial conditions

$$\psi_i(0) = \int_{\Omega_m} P_{0m} w_i, \quad \Psi_i(0) = \int_\gamma P_{0f} W_i.$$

The existence and uniqueness of P^n follows from the Carathéodory theory of ODEs. Multiplying (5.13) by ψ_i' and (5.14) by Ψ_i', summing over $i = 1, ..., n$ and integrating in time, we arrive at the identity

$$\left\| \partial_t (\sqrt{S_m} P^n_m, \sqrt{\delta S_f} P^n_f) \right\|^2_{\mathscr{L}} + \frac{1}{2} \frac{\mathrm{d}}{\mathrm{d}t} \left(\int_{\Omega_m} \mathbb{K}_m \nabla P^n_m \cdot \nabla P^n_m + \delta \int_\gamma \left\{\!\!\left\{ \mathbb{K}_f \widetilde{\nabla} P^n \cdot \widetilde{\nabla} P^n \right\}\!\!\right\} \right) = \left\langle \tilde{G}, \partial_t P^n \right\rangle_{\mathcal{V}}. \tag{5.15}$$

From the positive definiteness of $\mathbb{K}_f$ and the definition of $\widetilde{\nabla}^{\oplus}$ we infer that

$$\left\{\!\!\left\{ \mathbb{K}_f \widetilde{\nabla} P^n \cdot \widetilde{\nabla} P^n \right\}\!\!\right\} \geq \kappa_f |\nabla_\tau P_f^n|^2. \tag{5.16}$$

Hence, after integrating (5.15) in time, using the positive definiteness of $\mathbb{K}_m$, (5.16), the initial conditions and a suitable estimate of the right-hand side, we obtain:

$$\int_0^T \|\partial_t P^n\|_{\mathscr{L}}^2 + \sup_{t\in I} \|P^n\|_{\mathcal{V}}^2(t) \leq C \left(\|P_0\|_{\mathcal{V}}^2 + \int_0^T \left\|\tilde{G}\right\|_{\mathscr{L}}^2 \right), \tag{5.17}$$

where $C > 0$ may depend on $S_m, S_f, \delta, \kappa_m, \kappa_f, |\mathbb{K}_m|, |\mathbb{K}_f|$.

Hence the sequence $\{P^n\}_{n=1}^{\infty}$ is bounded in $\mathcal{X}$. Choosing a subsequence weakly convergent to an element P, we can pass to the limit in (5.13)–(5.14), which proves that P is a solution of (5.12).

Uniqueness: Let P^1 and P^2 be two solutions of (5.12) and denote their difference by ΔP. Subtracting the integral identities in (5.12b) for the two solutions and testing by ΔP we obtain:

$$\frac{1}{2}\frac{\mathrm{d}}{\mathrm{d}t} \left\| (\sqrt{S_m}\Delta P_m, \sqrt{\delta S_f}\Delta P_f) \right\|_{\mathscr{L}}^2 + \int_{\Omega_m} \mathbb{K}_m \nabla \Delta P_m \cdot \nabla \Delta P_m + \delta \int_\gamma \left\{\!\!\left\{ \mathbb{K}_f \widetilde{\nabla} \Delta P \cdot \widetilde{\nabla} \Delta P \right\}\!\!\right\} = 0. \tag{5.18}$$

Since all but the first term on the left hand side of (5.18) are nonnegative, we obtain the inequality

$$\frac{\mathrm{d}}{\mathrm{d}t} \|\Delta P\|_{\mathscr{L}}^2 \leq 0,$$

which together with the fact that $\Delta P(0,\cdot) = (0,0)$ implies $P^1 = P^2$. □

Having the above result, we introduce the solution map $\mathcal{F} : L^2(I;\mathscr{L}) \to \mathcal{X}$ by the relation

$$\mathcal{F}(\tilde{G}) := P,$$

where P is the solution of (5.12). Let $\boldsymbol{\beta} := (\beta_m, \beta_f)$ be a pair of positive parameters. We define a similar map $\mathcal{F}_{\boldsymbol{\beta}}$ as the solution operator for the flow problem with increased storativity $S_m + \beta_m$, $S_f + \beta_f$, respectively. In particular, $P := \mathcal{F}_{\boldsymbol{\beta}}(\tilde{G})$ satisfies the initial conditions (5.12a) and the integral identity

$$(S_m + \beta_m) \int_{\Omega_m} Q_m \partial_t P_m + \int_{\Omega_m} \mathbb{K}_m \nabla P_m \cdot \nabla Q_m + \delta(S_f + \beta_f) \int_\gamma Q_f \partial_t P_f + \delta \int_\gamma \left\{\!\!\left\{ \mathbb{K}_f \widetilde{\nabla} P \cdot \widetilde{\nabla} Q \right\}\!\!\right\} = \left\langle \tilde{G}, Q \right\rangle_{\mathscr{L}} \tag{5.19}$$

for all $Q := (Q_m, Q_f) \in \mathcal{V}$ and a.a. $t \in I$.

5.3 Fixed-stress iterations

To prove the existence and uniqueness of the solution to (5.2), we follow the idea of optimized fixed-stress splitting from [32]. For any $n \in \{0, 1, 2, ...\}$ and $P^n \in \mathcal{X}$ we define

$$\mathbf{U}^n := \mathcal{E}(P^n).$$

Next we choose a pair of positive parameters $\boldsymbol{\beta} := (\beta_m, \beta_f)$ and define

$$P^{n+1} := \mathcal{F}_{\boldsymbol{\beta}}(\tilde{G}^n),$$

where

$$\begin{aligned}\tilde{G}_m^n &:= G_m - \alpha_m \operatorname{div} \partial_t \mathbf{U}_m^n + \beta_m \partial_t P_m^n,\\ \tilde{G}_f^n &:= G_f - \delta\alpha_f \left\{\!\!\left\{ \widetilde{\operatorname{div}} \partial_t \mathbf{U}^n \right\}\!\!\right\} + \delta\beta_f \partial_t P_f^n.\end{aligned}$$

From the results of sections 5.1 and 5.2 we infer that whenever $G \in L^2(I;\mathscr{L})$ then also $\tilde{G}^n := (\tilde{G}_m^n, \tilde{G}_f^n) \in L^2(I;\mathscr{L})$. The above scheme defines the mapping

$$\mathcal{M}_{\boldsymbol{\beta}} : P^n \mapsto P^{n+1}$$

from $\mathcal{X}$ into itself. If $\hat{P}$ is a fixed point of this map and $\hat{\mathbf{U}} := \mathcal{E}(\hat{P})$, then $(\hat{\mathbf{U}}, \hat{P})$ is a solution to (5.2). Let

$$\omega := \min\left\{ \frac{S_m + \beta_m}{\beta_m}, \frac{S_f + \beta_f}{\beta_f} \right\}.$$

Then the following expression $\rho_{\boldsymbol{\beta}}$ is a distance in $\mathcal{X}$:

$$\begin{aligned}\rho_{\boldsymbol{\beta}}(P_1, P_2)^2 := \frac{\omega}{\beta_m} \int_0^T \left\| \partial_t \left(\alpha_m \operatorname{div}(\mathbf{U}_{m1} - \mathbf{U}_{m2}) - \beta_m (P_{m1} - P_{m2}) \right) \right\|_{L^2(\Omega_m)}^2 \\ + \frac{\delta\omega}{\beta_f} \int_0^T \left\{\!\!\left\{ \left\| \partial_t \left(\alpha_f \widetilde{\operatorname{div}}(\mathbf{U}_1 - \mathbf{U}_2) - \beta_f (P_{f1} - P_{f2}) \right) \right\|_{L^2(\gamma)}^2 \right\}\!\!\right\} \\ + \sup_{t\in I} \left(\kappa_m \left\| \nabla(P_{m1} - P_{m2}) \right\|_{L^2(\Omega_m)}^2 + \delta\kappa_f \left\{\!\!\left\{ \left\| \widetilde{\nabla}(P_1 - P_2) \right\|_{L^2(\gamma)}^2 \right\}\!\!\right\} \right),\end{aligned}$$

where $\mathbf{U}_i := \mathcal{E}(P_i)$, $i = 1, 2$. Further, $(\mathcal{X}, \rho_{\boldsymbol{\beta}})$ is a complete metric space. We shall prove that $\mathcal{M}_{\boldsymbol{\beta}}$ is a contraction with respect to $\rho_{\boldsymbol{\beta}}$. Then $\mathcal{M}_{\boldsymbol{\beta}}$ has a unique fixed point and (5.2) has a unique solution, thus Theorem 5.1 will be proved.

Theorem 5.8. *Let $\mathbf{F} \in H^1(I;\boldsymbol{\mathcal{V}}^*)$, $G \in L^2(I;\mathscr{L})$ and $P_0 \in \mathcal{V}$. If the pair $\boldsymbol{\beta} = (\beta_m, \beta_f)$ satisfies*

$$\beta_m \geq \frac{\alpha_m^2}{2\left(\frac{2\mu_m}{d} + \lambda_m\right)} \quad \text{and} \quad \beta_f \geq \frac{\alpha_f^2}{2\left(\frac{2\mu_f}{d} + \lambda_f\right)}, \tag{5.20}$$

then $\mathcal{M}_{\boldsymbol{\beta}}$ is a contraction in $\mathcal{X}$ with respect to the distance $\rho_{\boldsymbol{\beta}}$. Hence, the sequence $\{P^n\}_{n=0}^{\infty}$ with an arbitrary initial guess $P^0 \in \mathcal{X}$, has a unique fixed point $\hat{P}$. Denoting $\hat{\mathbf{U}} := \mathcal{E}(\hat{P})$, then $(\hat{\mathbf{U}}, \hat{P})$ is the unique solution of the coupled problem (5.2). The contraction constant takes the value $1/\omega$, which becomes smallest when the equalities hold in (5.20).

Proof. For $n = 1, 2, \ldots$ we denote:

$$\Delta_P^n := P^n - P^{n-1}, \quad e_P^n := \partial_t \Delta_P^n, \quad \mathbf{e}_{\mathbf{U}}^n := \partial_t(\mathbf{U}^n - \mathbf{U}^{n-1}).$$

We subtract the equations (5.11) for $\partial_t \mathbf{U}^{n+1}$ and $\partial_t \mathbf{U}^n$ and test by $\mathbf{e}_{\mathbf{U}}^{n+1}$. We obtain:

$$\int_{\Omega_m} \mathbb{C}_m \nabla \mathbf{e}_{\mathbf{U}m}^{n+1} : \nabla \mathbf{e}_{\mathbf{U}m}^{n+1} + \delta \int_\gamma \left\{\!\!\left\{ \mathbb{C}_f \widetilde{\nabla} \mathbf{e}_{\mathbf{U}}^{n+1} : \widetilde{\nabla} \mathbf{e}_{\mathbf{U}}^{n+1} \right\}\!\!\right\}$$
$$= \int_{\Omega_m} e_{Pm}^{n+1} \alpha_m \operatorname{div} \mathbf{e}_{\mathbf{U}m}^{n+1} + \delta \int_\gamma e_{Pf}^{n+1} \left\{\!\!\left\{ \alpha_f \widetilde{\operatorname{div}} \mathbf{e}_{\mathbf{U}}^{n+1} \right\}\!\!\right\}.$$

Using (2.2) and the inequalities (A.1)–(A.2) from appendix A we obtain:

$$\left(\frac{2\mu_m}{d} + \lambda_m\right) \left\|\operatorname{div} \mathbf{e}_{\mathbf{U}m}^{n+1}\right\|_{L^2(\Omega_m)}^2 + \delta \left(\frac{2\mu_f}{d} + \lambda_f\right) \left\{\!\!\left\{ \left\|\widetilde{\operatorname{div}} \mathbf{e}_{\mathbf{U}}^{n+1}\right\|_{L^2(\gamma)}^2 \right\}\!\!\right\}$$
$$\leq \int_{\Omega_m} e_{Pm}^{n+1} \alpha_m \operatorname{div} \mathbf{e}_{\mathbf{U}m}^{n+1} + \delta \int_\gamma e_{Pf}^{n+1} \left\{\!\!\left\{ \alpha_f \widetilde{\operatorname{div}} \mathbf{e}_{\mathbf{U}}^{n+1} \right\}\!\!\right\},$$

which together with (5.20) yields:

$$\frac{1}{2\beta_m} \left\|\alpha_m \operatorname{div} \mathbf{e}_{\mathbf{U}m}^{n+1}\right\|_{L^2(\Omega_m)}^2 + \frac{\delta}{2\beta_f} \left\{\!\!\left\{ \left\|\alpha_f \widetilde{\operatorname{div}} \mathbf{e}_{\mathbf{U}}^{n+1}\right\|_{L^2(\gamma)}^2 \right\}\!\!\right\}$$
$$- \frac{1}{\beta_m} \int_{\Omega_m} \beta_m e_{Pm}^{n+1} \alpha_m \operatorname{div} \mathbf{e}_{\mathbf{U}m}^{n+1} - \frac{\delta}{\beta_f} \int_\gamma \beta_f e_{Pf}^{n+1} \alpha_f \left\{\!\!\left\{ \widetilde{\operatorname{div}} \mathbf{e}_{\mathbf{U}}^{n+1} \right\}\!\!\right\} \leq 0. \quad (5.21)$$

Next we subtract the equations (5.19) for P^{n+1} and P^n with appropriate right-hand sides $\tilde{G}^n$ and $\tilde{G}^{n-1}$, respectively, test by e_P^{n+1}, integrate in time and use (2.3), which yields for a.a. $t \in I$:

$$(S_m + \beta_m) \int_0^t \left\|e_{Pm}^{n+1}\right\|_{L^2(\Omega_m)}^2 + \delta(S_f + \beta_f) \int_0^t \left\|e_{Pf}^{n+1}\right\|_{L^2(\gamma)}^2$$
$$+ \frac{\kappa_m}{2} \left\|\nabla \Delta_{Pm}^{n+1}\right\|_{L^2(\Omega_m)}^2(t) + \frac{\delta \kappa_f}{2} \left\{\!\!\left\{ \left\|\widetilde{\nabla} \Delta_P^{n+1}\right\|_{L^2(\gamma)}^2(t) \right\}\!\!\right\}$$
$$\leq - \int_0^t \int_{\Omega_m} \underbrace{\left(\alpha_m \operatorname{div} \mathbf{e}_{\mathbf{U}m}^n - \beta_m e_{Pm}^n\right)}_{=: e_\sigma^n} e_{Pm}^{n+1} - \delta \int_0^t \int_\gamma \left\{\!\!\left\{ \underbrace{\alpha_f \widetilde{\operatorname{div}} \mathbf{e}_{\mathbf{U}}^n - \beta_f e_{Pf}^n}_{=: e_\Sigma^n} \right\}\!\!\right\} e_{Pf}^{n+1}. \quad (5.22)$$

We apply Hölder's and Young's inequality to the right hand side of (5.22) and obtain:

$$\frac{S_m + \beta_m}{\beta_m^2} \int_0^t \left\|\beta_m e_{Pm}^{n+1}\right\|_{L^2(\Omega_m)}^2 + \delta \frac{S_f + \beta_f}{\beta_f^2} \int_0^t \left\|\beta_f e_{Pf}^{n+1}\right\|_{L^2(\gamma)}^2$$
$$+ \frac{\kappa_m}{2} \left\|\nabla \Delta_{Pm}^{n+1}\right\|_{L^2(\Omega_m)}^2(t) + \frac{\delta \kappa_f}{2} \left\{\!\!\left\{ \left\|\widetilde{\nabla} \Delta_P^{n+1}\right\|_{L^2(\gamma)}^2(t) \right\}\!\!\right\}$$
$$\leq \frac{S_m + \beta_m}{2\beta_m^2} \int_0^t \left\|\beta_m e_{Pm}^{n+1}\right\|_{L^2(\Omega_m)}^2 + \frac{1}{2(S_m + \beta_m)} \int_0^t \left\|e_\sigma^n\right\|_{L^2(\Omega_m)}^2$$
$$+ \frac{\delta(S_f + \beta_f)}{2\beta_f^2} \int_0^t \left\|\beta_f e_{Pf}^n\right\|_{L^2(\gamma)}^2 + \frac{\delta}{2(S_f + \beta_f)} \int_0^t \left\{\!\!\left\{ \left\|e_\Sigma^n\right\|_{L^2(\gamma)}^2 \right\}\!\!\right\}. \quad (5.23)$$

Subtracting the first and third term from the right-hand side of (5.23) and estimating the coefficients $(S_* + \beta_*)/\beta_*^2$ from below by ω/β_*, $* \in \{m, f\}$, the inequality simplifies as follows:

$$\begin{aligned}
&\frac{\omega}{2\beta_m}\int_0^t \left\|\beta_m e_{Pm}^{n+1}\right\|^2_{L^2(\Omega_m)} + \frac{\delta\omega}{2\beta_f}\int_0^t \left\|\beta_f e_{Pf}^{n+1}\right\|^2_{L^2(\gamma)} \\
&\qquad + \frac{\kappa_m}{2}\left\|\nabla\Delta_{Pm}^{n+1}\right\|^2_{L^2(\Omega_m)}(t) + \frac{\delta\kappa_f}{2}\left\{\!\!\left\{\left\|\widetilde{\nabla}\Delta_P^{n+1}\right\|^2_{L^2(\gamma)}(t)\right\}\!\!\right\} \\
&\qquad \le \frac{1}{2(S_m+\beta_m)}\int_0^t \|e_\sigma^n\|^2_{L^2(\Omega_m)} + \frac{\delta}{2(S_f+\beta_f)}\int_0^t \left\{\!\!\left\{\|e_\Sigma^n\|^2_{L^2(\gamma)}\right\}\!\!\right\}. \qquad (5.24)
\end{aligned}$$

Now we multiply (5.21) by ω, integrate in time and add to (5.24). The square of the difference formula then yields:

$$\begin{aligned}
&\frac{\omega}{2\beta_m}\int_0^t \left\|e_\sigma^{n+1}\right\|^2_{L^2(\Omega_m)} + \frac{\delta\omega}{2\beta_f}\int_0^t \left\{\!\!\left\{\left\|e_\Sigma^{n+1}\right\|^2_{L^2(\gamma)}\right\}\!\!\right\} \\
&\qquad + \frac{\kappa_m}{2}\left\|\nabla\Delta_{Pm}^{n+1}\right\|^2_{L^2(\Omega_m)}(t) + \frac{\delta\kappa_f}{2}\left\{\!\!\left\{\left\|\widetilde{\nabla}\Delta_P^{n+1}\right\|^2_{L^2(\gamma)}(t)\right\}\!\!\right\} \\
&\qquad\qquad \le \frac{1}{2(S_m+\beta_m)}\int_0^t \|e_\sigma^n\|^2_{L^2(\Omega_m)} + \frac{\delta}{2(S_f+\beta_f)}\int_0^t \left\{\!\!\left\{\|e_\Sigma^n\|^2_{L^2(\gamma)}\right\}\!\!\right\}.
\end{aligned}$$

Using the fact that $\frac{1}{S_*+\beta_*} \le \frac{1}{\omega^2}\frac{\omega}{\beta_*}$, $* \in \{m, f\}$, the right-hand side of the above inequality can be estimated from above and we obtain:

$$\begin{aligned}
&\frac{1}{2}\left(\rho_{\boldsymbol{\beta}}(P^{n+1}, P^n)\right)^2 \\
&\qquad \le \frac{1}{\omega^2}\left(\frac{\omega}{2\beta_m}\int_0^t \|e_\sigma^n\|^2_{L^2(\Omega_m)} + \frac{\delta\omega}{2\beta_f}\int_0^t \left\{\!\!\left\{\|e_\Sigma^n\|^2_{L^2(\gamma)}\right\}\!\!\right\}\right) \\
&\qquad\qquad \le \frac{1}{2\omega^2}\left(\rho_{\boldsymbol{\beta}}(P^n, P^{n-1})\right)^2.
\end{aligned}$$

Hence

$$\rho_{\boldsymbol{\beta}}(P^{n+1}, P^n) \le \frac{1}{\omega}\rho_{\boldsymbol{\beta}}(P^n, P^{n-1}).$$

It is readily seen that $\omega > 1$. Since ω is non-increasing with respect to β_m and β_f, the smallest constant of contraction is obtained for the smallest possible values of β_m, β_f. □

As we have noted above, Theorem 5.8 implies the existence of a unique solution to (5.2). Hence Theorem 5.1 is proved.

Remark 5.1. *Since the problem (5.2) is linear, one could also use a direct method for proving its well-posedness. In particular, the Lax-Milgram theorem might be applied to the time-discretized coupled problem and the appropriate uniform bounds could be derived using an analogous approach as for the energy estimate. The benefit of Theorem 5.8 is the explicit rate of convergence for the iterative splitting that can be useful for the numerical simulations.*

6 Computational example

The aim of this section is to demonstrate the relevance of the DFM poroelasticity model by applying it to a simple test problem, and verify the convergence of the iterative splitting.

6.1 Description of test problem

We choose a problem of fluid injection into a one dimensional fracture, which is located in the middle of a block of impermeable rock. The injection pressure causes a sudden opening and propagation of the pressure in the fracture. The setting of the test is chosen to mimic the analytical similarity solution from [42], see also [41].

The computational domain is the rectangle $(0, L) \times (0, H)$, $L = 25$ m, $H = 1$ m, with the fracture line $(0, L) \times \{\frac{H}{2}\}$. Initially, there is a uniform fluid pressure $p_0 = 11$ MPa in the whole domain. During the test, the fluid is injected at the left fracture end under the pressure $p_{in} = 11.9$ MPa, while at the right end the pressure is kept at the initial value p_0. The boundary of the rectangle is impermeable. For the mechanical part, we set zero displacement condiction on the bottom side of the domain, the left and right sides and the fracture ends are subject to the roller boundary condition $\mathbf{U}_{\{m,f\}} \cdot \mathbf{n} = 0$ and the top side is under constant traction of 11 MPa. The geometry and the boundary conditions are depicted in Figure 2.

We consider both the rock and the fracture to be isotropic, i.e.

$$\mathbb{K}_* = \frac{k_*}{\mu}\mathbb{I}, \quad \mathbb{C}_*\nabla\mathbf{U} = \frac{E_*}{1+\nu_*}\varepsilon(\mathbf{U}) + \frac{E_*\nu_*}{(1+\nu_*)(1-2\nu_*)}(\operatorname{div}\mathbf{U})\mathbb{I}, \ * \in \{m, f\}, \tag{6.1}$$

denoting by μ the viscosity of the fluid and by E_*, ν_* the Young modulus and the Poisson ratio of the rock matrix and fracture, respectively. The model parameters are given in Table 1.

Assuming an infinite fracture and perfectly impermeable rock, a closed-form solution can be found for the problem. In particular, the formula (21) in [42] gives rise to the following expression of fracture pressure:

$$P_f(t, x) = p_0 + (p_{in} - p_0)\operatorname{erfc}\left(\sqrt{\frac{\mu(1+\nu_f)}{2k_f E_f}}\frac{x}{\sqrt{t}}\right), \tag{6.2}$$

where the fracture permeability satisfies the cubic law $k_f = \delta^2/12$ and the fracture stiffness is given by the ratio of the shear modulus and the cross-section. The formula (6.2) will be used to validate the numerical solution described in the next subsection.

6.2 Numerical solution

The numerical scheme of the discrete fracture-matrix model has been implemented as part of the Flow123d simulator [15], which uses conforming simplicial mixed meshes. The flow part of the problem is discretized using the implicit Euler timestepping and the lumped mixed hybrid finite element method [43].

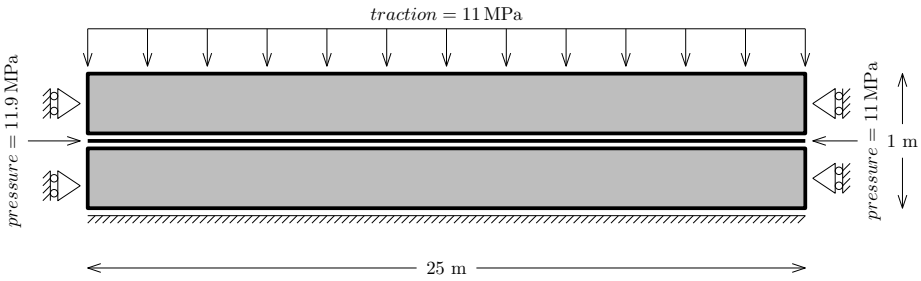

Figure 2: Geometry and boundary conditions for the test problem.

Parameter	Value	
	Matrix	**Fracture**
k [m^2]	10^{-21}	8.3×10^{-12}
μ [Pa s]	10^{-3}	10^{-3}
S [Pa^{-1}]	10^{-12}	10^{-10}
E [Pa]	60×10^9	10^6
ν [−]	0	0
α [−]	1	1
δ [m]	—	10^{-5}

Table 1: Parameters for the test problem.

The mechanical part is discretized using linear finite elements for the displacement. In each discrete time, the coupled hydro-mechanical problem is solved iteratively using the fixed-stress splitting. The iterations are stopped when the relative difference of two successive iterates drops below the given tolerance:

$$\left\| P^n - P^{n-1} \right\|_{\mathscr{L}} \leq tol \left\| P^{n-1} \right\|_{\mathscr{L}}. \tag{6.3}$$

We refer to [15] for further details of the implementation.

6.3 Results and discussion

For the test problem, the computational mesh consists of 6856 triangular elements, and the fracture is divided into 500 lines, which coincide with sides of adjacent triangular elements. The computational time interval is $[0, 2000\,\mathrm{s}]$ with the time step $\Delta t = 100\,\mathrm{s}$. The computed pressure profile in the fracture at selected times is depicted and compared to the analytical solution in Figure 3. The results are in a good agreement.

Next, we test the iterative coupling of flow and mechanics. Motivated by Theorem 5.8, we set

$$\beta_* := \tilde{\beta} \frac{\alpha_*^2}{2(\mu_* + \lambda_*)}, \ * \in \{m, f\}, \tag{6.4}$$

where $\tilde{\beta} \in [0.3, 10]$ is a scaling parameter, and study its influence on the convergence of the coupling. The tolerance for the iterations is set to $tol = 10^{-6}$. In Figure 4a we show the dependence of number of iterations, necessary to achieve the convergence criterion, on $\tilde{\beta}$. The number of iterations was averaged over

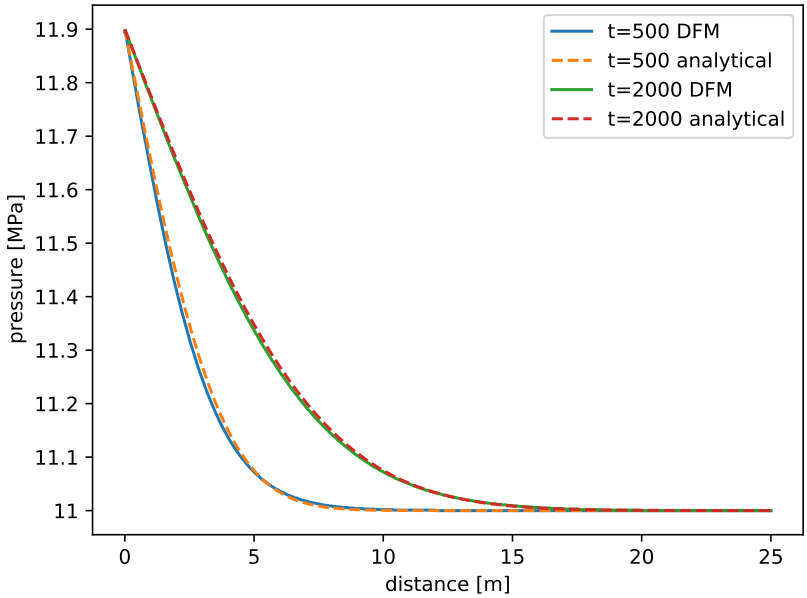

Figure 3: Comparison of fracture pressure given by the DFM model and by the analytical solution.

all time steps and depicted together with the range between the minimal and maximal values. It turns out that, in agreement with Theorem 5.8, the optimal value of $\tilde{\beta}$ is close to 1. Moreover, its overestimation leads to moderate increase of number of iterations while for $\tilde{\beta} < 1$ the iterative scheme converges very slowly or diverges. To verify the robustness of the estimate (5.20), we performed analogous tests for perturbed conductivity, and elastic moduli, see Figure 4. From the results it can be seen that the optimal choice of $\tilde{\beta}$ is in all cases either 1 or slightly larger, which confirms the theoretical estimates.

Conclusion

We have derived a DFM model of flow and linear elasticity in fractured porous media. The model was derived from physical principles expressed by the Biot system and takes into account possible anisotropy of the hydraulic conductivity and elasticity tensors. A simplified geometry consisting of one straight fracture was considered.

Under the assumption of permeable fracture, the existence and uniqueness of weak solution was proved. The proof was based on the fixed-stress splitting scheme for which the convergence has been analyzed and optimal values of iteration parameters were found in as similar form as in [12].

A numerical test was presented that confirmed the theoretical convergence result of the splitting scheme as well as the applicability of the DFM model. The analysis of the numerical scheme is beyond the scope of the present paper.

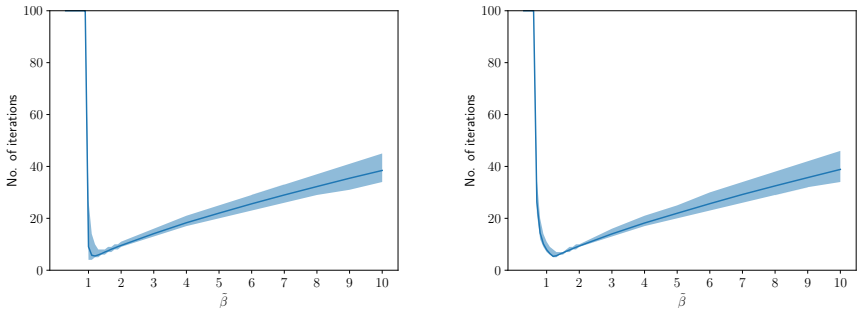

(a) Parameters from Table 1.

(b) $k_m = 10^{-14}$

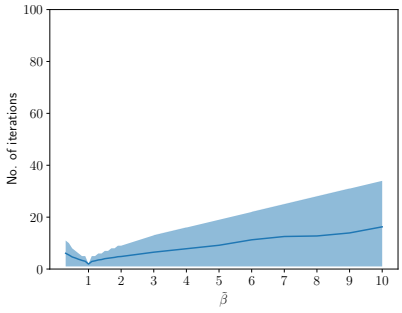

(c) $k_m = 10^{-8}$

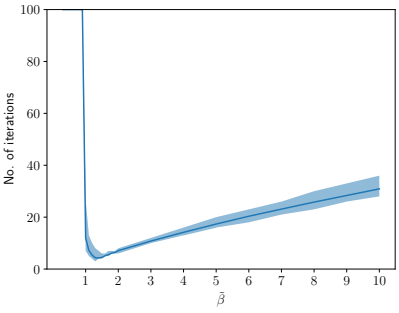

(d) $\nu_m = \nu_f = 0.25$

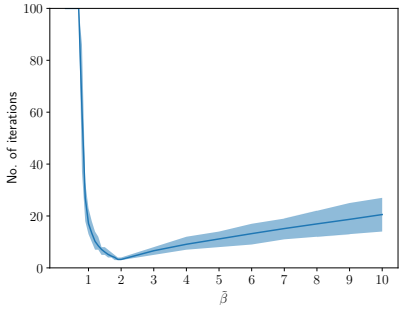

(e) $\nu_m = \nu_f = 0.49$

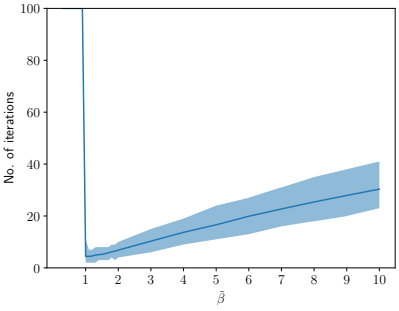

(f) $E_f = 10^9$

Figure 4: Convergence of iterative splitting. Number of iterations necessary for meeting the stopping criterion is depicted for several parameter cases. The filled area indicates the range of iteration counts for all time steps, the line shows the average number of iterations.

The model can be extended in many directions, namely to more complex geometries (embedded fractures with variable aperture and their intersections), nonlinear fracture mechanics, or variable fracture permeability, to name a few challenging tasks. Some of these have been implemented in the Flow123d simulator, others are a subject of ongoing research. Nonlinear poroelastic couplings such as in [10, 11] can also be considered, requiring possibly a more advanced splitting or linearization approach.

Acknowledgement

The research was supported by the Euratom research and training programme 2014-2018 under grant agreement No [847593].

Appendix A. Auxiliary inequalities and identities

In what follows we prove some technical relations that are used in the paper.

Lemma A.1. *For all admissible functions f, $\mathbf{v}$ and $\mathbb{A}$ it holds:*

$$\begin{aligned}
\overline{\nabla f} &= \nabla_\tau \overline{f} + \frac{1}{\delta}\,[\![f]\!]\,\boldsymbol{\nu} = \left\{\!\!\left\{\widetilde{\nabla}(f,\overline{f})\right\}\!\!\right\},\\
\overline{\nabla \mathbf{v}} &= \nabla_\tau \overline{\mathbf{v}} + \frac{1}{\delta}\,[\![\mathbf{v}]\!]\otimes\boldsymbol{\nu} = \left\{\!\!\left\{\widetilde{\nabla}(\mathbf{v},\overline{\mathbf{v}})\right\}\!\!\right\},\\
\overline{\operatorname{div}\mathbf{v}} &= \operatorname{div}_\tau \overline{\mathbf{v}} + \frac{1}{\delta}\,[\![\mathbf{v}]\!]\cdot\boldsymbol{\nu} = \left\{\!\!\left\{\widetilde{\operatorname{div}}(\mathbf{v},\overline{\mathbf{v}})\right\}\!\!\right\},\\
\overline{\operatorname{div}\mathbb{A}} &= \operatorname{div}_\tau \overline{\mathbb{A}} + \frac{1}{\delta}\,[\![\mathbb{A}^\top]\!]\,\boldsymbol{\nu}.
\end{aligned}$$

Proof. It is readily seen that $\left\{\!\!\left\{\widetilde{\nabla}(f,\overline{f})\right\}\!\!\right\} = \nabla_\tau\overline{f} + \frac{1}{\delta}[\![f]\!]$. Further we have:

$$\overline{\nabla_\tau f} = \frac{1}{\delta}\int_{-\frac{\delta}{2}}^{\frac{\delta}{2}} \nabla_\tau f(\cdot + s\boldsymbol{\nu})\,\mathrm{d}s = \nabla_\tau\left(\frac{1}{\delta}\int_{-\frac{\delta}{2}}^{\frac{\delta}{2}} f(\cdot+s\boldsymbol{\nu})\,\mathrm{d}s\right) = \nabla_\tau\overline{f},$$

$$\overline{\nabla_\nu f} = \frac{1}{\delta}\int_{-\frac{\delta}{2}}^{\frac{\delta}{2}} \boldsymbol{\nu}\frac{\mathrm{d}}{\mathrm{d}s}\left(f(\cdot+s\boldsymbol{\nu})\right)\,\mathrm{d}s = \frac{1}{\delta}\,[\![f]\!]\,\boldsymbol{\nu},$$

so that $\overline{\nabla f} = \overline{\nabla_\tau f} + \overline{\nabla_\nu f} = \left\{\!\!\left\{\widetilde{\nabla}(f,\overline{f})\right\}\!\!\right\}$. The remaining identities can be proved analogously. □

Lemma A.2. *For all functions $\mathbf{V} := (\mathbf{V}_m, \mathbf{V}_f) \in \boldsymbol{\mathcal{V}}$ it holds:*

$$\|\operatorname{div}\mathbf{V}_m\|^2_{L^2(\Omega_m)} \le d\,\|\boldsymbol{\varepsilon}(\mathbf{V}_m)\|^2_{L^2(\Omega_m)}\,, \tag{A.1}$$

$$\left\|\widetilde{\operatorname{div}}^{\oplus}\mathbf{V}\right\|^2_{L^2(\gamma)} \le d\,\left\|\tilde{\boldsymbol{\varepsilon}}^{\oplus}(\mathbf{V})\right\|^2_{L^2(\gamma)}\,. \tag{A.2}$$

Proof. For any tensor $\mathbb{A} \in \mathbf{R}^{d\times d}$, the AM-QM inequality implies

$$|\mathbb{I} : \mathbb{A}|^2 \leq d|\mathbb{A}|^2.$$

Choosing $\mathbb{A} := \boldsymbol{\varepsilon}(\mathbf{V}_m)$ and integrating the inequality over Ω_m we obtain (A.1). Similarly, (A.2) is obtained for $\mathbb{A} := \widetilde{\boldsymbol{\varepsilon}}^{\oplus}(\mathbf{V})$ and integration over γ. □

Lemma A.3. *The functions* $\mathbf{t}^{\oplus}$ *and* $\varphi^{\oplus}$*, defined in* (4.1) *and* (4.6)*, satisfy:*

$$[\![\mathbf{t}(\mathbf{V}) \cdot (\mathbf{W}_m - \mathbf{W}_f)]\!] = \delta \left\{\!\!\left\{ \mathbb{C}_f \widetilde{\nabla}\mathbf{V} : \widetilde{\nabla}_\nu \mathbf{W} \right\}\!\!\right\}, \tag{A.3}$$

$$[\![\varphi(Q)(R_m - R_f)]\!] = \delta \left\{\!\!\left\{ \mathbb{K}_f \widetilde{\nabla} Q \cdot \widetilde{\nabla}_\nu R \right\}\!\!\right\} \tag{A.4}$$

for all admissible functions $\mathbf{V} := (\mathbf{V}_m, \mathbf{V}_f)$, $\mathbf{W} := (\mathbf{W}_m, \mathbf{W}_f)$, $Q := (Q_m, Q_f)$ *and* $R := (R_m, R_f)$.

Proof. From the definition of $\mathbf{t}^{\oplus}$ and $\widetilde{\nabla}^{\oplus}$ it follows that

$$\begin{aligned}\mathbf{t}^{\oplus}(\mathbf{V}) \cdot (\mathbf{W}_m^{\oplus} - \mathbf{W}_f) = \pm\frac{\delta}{2}\mathbb{C}_f \widetilde{\nabla}^{\oplus}\mathbf{V} : \left(\pm\frac{2}{\delta}\right)(\mathbf{W}_m^{\oplus} - \mathbf{W}_f) \otimes \boldsymbol{\nu} \\ = \pm\frac{\delta}{2}\mathbb{C}_f \widetilde{\nabla}^{\oplus}\mathbf{V} : \widetilde{\nabla}_\nu^{\oplus}\mathbf{W}.\end{aligned}$$

Taking the jump of the above expression then yields (A.3). The second identity can be proved in analogous way. □

Appendix B. Weak formulation of (4.9)

In what follows we derive the integral identities (5.2b) – (5.2c). Multiplying (4.9a) and (4.9c) by test functions $\mathbf{V}_m$, $\mathbf{V}_f$, respectively, where $\mathbf{V} := (\mathbf{V}_m, \mathbf{V}_f) \in \boldsymbol{\mathcal{V}}$, integrating them by parts, summing and applying the boundary conditions (4.9g), we arrive at the identity

$$\begin{aligned}\int_{\Omega_m} (\mathbb{C}_m \nabla \mathbf{U}_m : \nabla \mathbf{V}_m - \alpha_m P_m \operatorname{div} \mathbf{V}_m) + \int_\gamma [\![(\mathbb{C}_m \nabla \mathbf{U}_m - \alpha_m P_m \mathbb{I})\boldsymbol{\nu} \cdot \mathbf{V}_m]\!] \\ + \delta \int_\gamma \mathbb{C}_f \left\{\!\!\left\{ \widetilde{\nabla}\mathbf{U} \right\}\!\!\right\} : \nabla_\tau \mathbf{V}_f - \int_\gamma \alpha_f \delta P_f \operatorname{div}_\tau \mathbf{V}_f - \int_\gamma [\![\mathbf{t}(\mathbf{U}) \cdot \mathbf{V}_f]\!] \\ = \langle \mathbf{F}, \mathbf{V} \rangle_{\boldsymbol{\mathcal{V}}}.\end{aligned} \tag{B.1}$$

The second term in (B.1) can be rewritten using the interface conditions (4.9e), which yields:

$$\begin{aligned}\int_{\Omega_m} (\mathbb{C}_m \nabla \mathbf{U}_m : \nabla \mathbf{V}_m - \alpha_m P_m \operatorname{div} \mathbf{V}_m) + \delta \int_\gamma \mathbb{C}_f \left\{\!\!\left\{ \widetilde{\nabla}\mathbf{U} \right\}\!\!\right\} : \nabla_\tau \mathbf{V}_f \\ + \int_\gamma [\![\mathbf{t}(\mathbf{U}) \cdot (\mathbf{V}_m - \mathbf{V}_f)]\!] - \delta \int_\gamma \alpha_f P_f \left\{\!\!\left\{ \widetilde{\operatorname{div}}\mathbf{V} \right\}\!\!\right\} = \langle \mathbf{F}, \mathbf{V} \rangle_{\boldsymbol{\mathcal{V}}}.\end{aligned} \tag{B.2}$$

Using (A.3), we can rewrite (B.2) as follows:

$$\int_{\Omega_m} (\mathbb{C}_m \nabla \mathbf{U}_m : \nabla \mathbf{V}_m - \alpha_m P_m \operatorname{div} \mathbf{V}_m) + \delta \int_\gamma \left\{\!\!\left\{ \mathbb{C}_f \widetilde{\nabla} \mathbf{U} : \widetilde{\nabla} \mathbf{V} - \alpha_f P_f \widetilde{\operatorname{div}} \mathbf{V} \right\}\!\!\right\} = \langle \mathbf{F}, \mathbf{V} \rangle_{\boldsymbol{\mathcal{V}}},$$

which is (5.2b). Similarly, multiplying the equations (4.9b), (4.9d) by test functions Q_m, Q_f, respectively, where $Q := (Q_m, Q_f) \in \mathcal{V}$, integrating them by parts, and applying the boundary conditions (4.9g), we obtain:

$$\int_{\Omega_m} (Q_m \partial_t (S_m P_m + \alpha_m \operatorname{div} \mathbf{U}_m) + \mathbb{K}_m \nabla P_m \cdot \nabla Q_m) + \int_\gamma [\![\mathbb{K}_m \nabla P_m \cdot \boldsymbol{\nu} Q_m]\!] + \delta \int_\gamma Q_f \partial_t \left(S_f P_f + \alpha_f \left\{\!\!\left\{ \widetilde{\operatorname{div}} \mathbf{U} \right\}\!\!\right\} \right) + \delta \int_\gamma \mathbb{K}_f \left\{\!\!\left\{ \widetilde{\nabla} P \right\}\!\!\right\} \cdot \nabla_\tau Q_f - \int_\gamma [\![\varphi(P)]\!] Q_f = \langle G, Q \rangle_{\mathscr{L}}.$$

Application of the interface conditions (4.9f) then gives rise to the identity

$$\int_{\Omega_m} (Q_m \partial_t (S_m P_m + \alpha_m \operatorname{div} \mathbf{U}_m) + \mathbb{K}_m \nabla P_m \cdot \nabla Q_m) + \delta \int_\gamma Q_f \partial_t \left(S_f P_f + \alpha_f \left\{\!\!\left\{ \widetilde{\operatorname{div}} \mathbf{U} \right\}\!\!\right\} \right) + \delta \int_\gamma \mathbb{K}_f \left\{\!\!\left\{ \widetilde{\nabla} P \right\}\!\!\right\} \cdot \nabla_\tau Q_f + \int_\gamma [\![\varphi(P)(Q_m - Q_f)]\!] = \langle G, Q \rangle_{\mathscr{L}}. \quad \text{(B.3)}$$

Due to (A.4), (B.3) becomes

$$\int_{\Omega_m} (Q_m \partial_t (S_m P_m + \alpha_m \operatorname{div} \mathbf{U}_m) + \mathbb{K}_m \nabla P_m \cdot \nabla Q_m) + \delta \int_\gamma Q_f \partial_t \left(S_f P_f + \alpha_f \left\{\!\!\left\{ \widetilde{\operatorname{div}} \mathbf{U} \right\}\!\!\right\} \right) + \delta \int_\gamma \left\{\!\!\left\{ \mathbb{K}_f \widetilde{\nabla} P \cdot \widetilde{\nabla} Q \right\}\!\!\right\} = \langle G, Q \rangle_{\mathscr{L}},$$

which is (5.2c).

The energy equality (5.1) can be obtained from the weak formulation as follows. One has to differentiate (5.2b) with respect to time, test by $\mathbf{V} := \partial_t \mathbf{U}$ and add to (5.2c) tested by $Q := \partial_t P$.

References

[1] P. Angot, F. Boyer, and F. Hubert. Asymptotic and numerical modelling of flows in fractured porous media. ESAIM: Mathematical Modelling and Numerical Analysis, 43(2):239–275, 2009.

[2] S. Bandis, A. Lumsden, and N. Barton. Fundamentals of rock joint deformation. International Journal of Rock Mechanics and Mining Sciences & Geomechanics Abstracts, 20(6):249–268, 1983.

[3] R. L. Berge, I. Berre, E. Keilegavlen, J. M. Nordbotten, and B. Wohlmuth. Finite volume discretization for poroelastic media with fractures modeled by contact mechanics. International Journal for Numerical Methods in Engineering, 2019.

[4] I. Berre, F. Doster, and E. Keilegavlen. Flow in fractured porous media: a review of conceptual models and discretization approaches. Transport in Porous Media, 130(1):215–236, 2019.

[5] M. A. Biot. General theory of three-dimensional consolidation. Journal of Applied Physics, 12(2):155–164, 1941.

[6] R. Blaheta, M. Béreš, S. Domesová, and D. Horák. Bayesian inversion for steady flow in fractured porous media with contact on fractures and hydro-mechanical coupling. Computational Geosciences, 24:1911–1932, 2020.

[7] F. Bonaldi, J. Droniou, and R. Masson. Numerical analysis of a mixed-dimensional poromechanical model with frictionless contact at matrix-fracture interfaces, 2022. URL https://arxiv.org/abs/2201.09646.

[8] E. Bonnet, O. Bour, N. E. Odling, P. Davy, I. Main, P. Cowie, and B. Berkowitz. Scaling of fracture systems in geological media. Reviews of Geophysics, 39(3):347–383, 2001. ISSN 1944-9208. doi: 10.1029/1999RG000074.

[9] W. Boon and J. M. Nordbotten. Mixed-dimensional poromechanical models of fractured porous media. Acta Mechanica, 234:1–48, 12 2022. doi: 10.1007/s00707-022-03378-1.

[10] M. Borregales, F. A. Radu, K. Kumar, and J. M. Nordbotten. Robust iterative schemes for non-linear poromechanics. Computational Geosciences, 22:1021–1038, 2018.

[11] M. A. Borregales Reverón, K. Kumar, J. M. Nordbotten, and F. A. Radu. Iterative solvers for biot model under small and large deformations. Computational Geosciences, 25:687–699, 2021.

[12] J. W. Both, M. Borregales, J. M. Nordbotten, K. Kumar, and F. A. Radu. Robust fixed stress splitting for Biot's equations in heterogeneous media. Applied Mathematics Letters, 68:101–108, 2017.

[13] J. Březina and J. Stebel. Analysis of model error for a continuum-fracture model of porous media flow. In High Performance Computing in Science and Engineering, Lecture Notes in Computer Science, pages 152–160. Springer, 2016.

[14] M. Bukač, I. Yotov, and P. Zunino. Dimensional model reduction for flow through fractures in poroelastic media. ESAIM: Mathematical Modelling and Numerical Analysis, 51(4):1429–1471, 2017.

[15] J. Březina, J. Stebel, D. Flanderka, and P. Exner. Flow123d – simulator of fractured porous media processes, 2022. URL http://flow123d.github.io.

[16] L. C. Evans. Partial differential equations, volume 19. American Mathematical Society, 2010.

[17] S. Follin, L. Hartley, I. Rhén, P. Jackson, S. Joyce, D. Roberts, and B. Swift. A methodology to constrain the parameters of a hydrogeological discrete fracture network model for sparsely fractured crystalline rock, exemplified by data from the proposed high-level nuclear waste repository site at Forsmark, Sweden. Hydrogeology Journal, 22(2):313–331, Mar. 2014. ISSN 1435-0157. doi: 10.1007/s10040-013-1080-2.

[18] L. Formaggia, A. Fumagalli, A. Scotti, and P. Ruffo. A reduced model for Darcy's problem in networks of fractures. ESAIM: Mathematical Modelling and Numerical Analysis, 48(4):1089–1116, 2014.

[19] A. Franceschini, N. Castelletto, J. A. White, and H. A. Tchelepi. Algebraically stabilized Lagrange multiplier method for frictional contact mechanics with hydraulically active fractures. Computer Methods in Applied Mechanics and Engineering, 368:113161, 2020.

[20] B. Ganis, V. Girault, M. Mear, G. Singh, and M. Wheeler. Modeling fractures in a poro-elastic medium. Oil & Gas Science and Technology–Revue d'IFP Energies nouvelles, 69(4):515–528, 2014.

[21] T. Garipov, M. Karimi-Fard, and H. Tchelepi. Discrete fracture model for coupled flow and geomechanics. Computational Geosciences, 20:149–160, 2016.

[22] V. Girault, M. Wheeler, B. Ganis, and M. Mear. A lubrication fracture model in a poro-elastic medium. Mathematical Models and Methods in Applied Sciences, pages 1–59, 09 2014. doi: 10.1142/S0218202515500141.

[23] V. Girault, M. F. Wheeler, K. Kumar, and G. Singh. Mixed formulation of a linearized lubrication fracture model in a poro-elastic medium. Contributions to Partial Differential Equations and Applications, pages 171–219, 2019.

[24] K. K. Hanowski and O. Sander. The hydromechanical equilibrium state of poroelastic media with a static fracture: A dimension-reduced model with existence results in weighted Sobolev spaces and simulations with an XFEM discretization. Mathematical Models and Methods in Applied Sciences, 28 (13):2511–2556, 2018.

[25] M. Hokr, H. Shao, W. Gardner, A. Balvín, H. Kunz, Y. Wang, and M. Vencl. Real-case benchmark for flow and tracer transport in the fractured rock. Environmental Earth Sciences, 75:1–17, 2016.

[26] J. D. Hyman, S. Karra, N. Makedonska, C. W. Gable, S. L. Painter, and H. S. Viswanathan. dfnWorks: A discrete fracture network framework for modeling subsurface flow and transport. Computers & Geosciences, 84: 10–19, Nov. 2015. ISSN 0098-3004. doi: 10.1016/j.cageo.2015.08.001.

[27] L. Jing and J. A. Hudson. Numerical methods in rock mechanics. International Journal of Rock Mechanics and Mining Sciences, 39(4):409–427, June 2002. ISSN 1365-1609. doi: 10.1016/S1365-1609(02)00065-5.

[28] L. Jing and O. Stephansson. 4 - Fluid Flow and Coupled Hydro-Mechanical Behavior of Rock Fractures. In L. Jing and O. Stephansson, editors, Developments in Geotechnical Engineering, volume 85 of Fundamentals of Discrete Element Methods for Rock Engineering, pages 111–144. Elsevier, Jan. 2007. doi: 10.1016/S0165-1250(07)85004-8.

[29] V. Martin, J. Jaffré, and J. E. Roberts. Modeling fractures and barriers as interfaces for flow in porous media. SIAM Journal on Scientific Computing, 26(5):1667, 2005.

[30] J. Maryška, O. Severýn, and M. Vohralík. Numerical simulation of fracture flow with a mixed-hybrid FEM stochastic discrete fracture network model. Computational Geosciences, 8(3):217–234, 2005.

[31] A. Mikelić and J. Tambača. Derivation of a poroelastic elliptic membrane shell model. Applicable Analysis, 98(1-2):136–161, 2019.

[32] A. Mikelić and M. F. Wheeler. Convergence of iterative coupling for coupled flow and geomechanics. Computational Geosciences, 17(3):455–461, 2013.

[33] M. Oda. An equivalent continuum model for coupled stress and fluid flow analysis in jointed rock masses. Water Resources Research, 22(13):1845–1856, 1986. ISSN 1944-7973. doi: 10.1029/WR022i013p01845.

[34] G. Pichot, J. Erhel, and J.-R. De Dreuzy. A generalized mixed hybrid mortar method for solving flow in stochastic discrete fracture networks. SIAM Journal on Scientific Computing, 34(1):B86–B105, 2012.

[35] J. Rutqvist and O. Stephansson. The role of hydromechanical coupling in fractured rock engineering. Hydrogeology Journal, 11(1):7–40, 2003.

[36] J. Rutqvist, C. Leung, A. Hoch, Y. Wang, and Z. Wang. Linked multicontinuum and crack tensor approach for modeling of coupled geomechanics, fluid flow and transport in fractured rock. Journal of Rock Mechanics and Geotechnical Engineering, 5(1):18–31, Feb. 2013. ISSN 1674-7755. doi: 10.1016/j.jrmge.2012.08.001.

[37] N. Schwenck, B. Flemisch, R. Helmig, and B. I. Wohlmuth. Dimensionally reduced flow models in fractured porous media: crossings and boundaries. Computational Geosciences, 19(6):1219–1230, 2015.

[38] R. E. Showalter. Diffusion in poro-elastic media. Journal of Mathematical Analysis and Applications, 251(1):310–340, 2000.

[39] J. Stebel, J. Kružík, D. Horák, J. Březina, and M. Béreš. On the parallel solution of hydro-mechanical problems with fracture networks and contact conditions, 2023. URL https://arxiv.org/abs/2311.13310.

[40] A. Vass, D. Koehn, R. Toussaint, I. Ghani, and S. Piazolo. The importance of fracture-healing on the deformation of fluid-filled layered systems. Journal of Structural Geology, 67:94–106, 2014. ISSN 0191-8141.

[41] N. Watanabe, W. Wang, J. Taron, U. Görke, and O. Kolditz. Lower-dimensional interface elements with local enrichment: application to coupled hydro-mechanical problems in discretely fractured porous media. International Journal for Numerical Methods in Engineering, 90(8):1010–1034, 2012.

[42] A. M. Wijesinghe. Exact similarity solution for coupled deformation and fluid flow in discrete fractures. Technical Report UCID-20675, Lawrence Livermore National Lab. (LLNL), Livermore, CA (United States), Feb. 1986.

[43] A. Younes, P. Ackerer, and F. Lehmann. A new mass lumping scheme for the mixed hybrid finite element method. International Journal for Numerical Methods in Engineering, 67(1):89–107, July 2006. ISSN 1097-0207. doi: 10.1002/nme.1628.

[44] A. Ženíšek. The existence and uniqueness theorem in Biot's consolidation theory. Aplikace Matematiky, 29(3):194–211, 1984.

[45] Z. Zhao, J. Rutqvist, C. Leung, M. Hokr, Q. Liu, I. Neretnieks, A. Hoch, J. Havlíček, Y. Wang, Z. Wang, Y. Wu, and R. Zimmerman. Impact of stress on solute transport in a fracture network: A comparison study. Journal of Rock Mechanics and Geotechnical Engineering, 5(2):110–123, Apr. 2013. ISSN 1674-7755. doi: 10.1016/j.jrmge.2013.01.002.